Bulletin of Volcanology (2022) 84: 95
https://doi.org/10.1007/s00445-022-01599-9

RESEARCH ARTICLE

Hydrovolcanic activity on a continental shelf inferred from the subsurface diatreme- and crater-filling deposits of Jeju Island, Korea

Yongmun Jeon[1] · Ki Hwa Park[2] · Young Kwan Sohn[1]

Received: 29 April 2022 / Accepted: 30 August 2022 / Published online: 24 September 2022

Abstract

Jeju Island comprises numerous tuff rings and tuff cones and their reworked deposits in the subsurface, which formed on the ca. 120-m-deep Yellow Sea continental shelf under the fluctuating Quaternary sea levels. Tens of meter-thick and massive deposits were found by chance during groundwater drilling at three sites. These deposits are interpreted as either syn-eruptive diatreme-filling deposits or post-eruptive crater-filling deposits, both of hydromagmatic volcanoes. The diatremes were cut into shelf sediment, 70 to 250 m thick, and developed generally within it below the Quaternary sea levels. Abundant external water was therefore available for explosive magma-water interactions at shallow levels. The diatreme deposit in one core shows some features attributable to extreme wetness or water saturation of the diatreme fill, such as the matrix support of larger clasts, meager vertical changes in matrix content, and an absence of features related to particle adhesion. Fluidally shaped clasts with delicate reentrant margins in the core suggest minimal particle abrasion and breakage in a water-saturated and highly fluid slurry of tephra and water that was probably filling a shallow bowl-like diatreme, which is distinguished from both phreatomagmatic and kimberlite diatremes. The diatreme deposits in other cores comprise blocky and angular clasts in a sideromelane ash matrix, suggesting phreatomagmatic explosions at a deeper level. One of the cores contains collapsed deposits of thinly stratified tuff emplaced by pyroclastic surges, indicating that the diatreme is associated with an emergent tuff ring. Both Surtseyan and phreatomagmatic eruptions are therefore interpreted to have occurred on the shelf under the controls of fluctuating Quaternary sea levels. The subsurface diatremes suggest that there can be a variety of diatremes with different sizes, shapes, and material characteristics beneath the craters of hydromagmatic volcanoes, including not only maars but also tuff rings and tuff cones.

Keywords Diatreme · Tuff ring · Tuff cone · Maar · Hydrovolcanism · Surtseyan eruption · Continental shelf

초록

제주도는 약 120 m 수심의 황해 대륙붕 위에서 제4기 해수면 변동의 영향을 받으며 형성되었고, 지하에는 무수한 응회환과 응회구 그리고 이들의 재동퇴적층이 나타난다. 지하수 개발을 위한 시추 도중 세 지점에서 수십 m 두께의 괴상층이 우연히 발견되었다. 이 층들은 수성화산 분화 당시 형성된 다이아트림과 분출 이후의 분화구를 채우고 있었던 것으로 해석된다. 이 다이아트림들은 대체로 제4기 해수면 아래에서 70~250 m의 두께를 지닌 대륙붕 퇴

Editorial responsibility: J.L. Smellie

Ki Hwa Park is deceased.

✉ Young Kwan Sohn
yksohn@gnu.ac.kr

[1] Department of Geology and Research Institute of Natural Science, Gyeongsang National University, Jinju 52828, Republic of Korea

[2] Groundwater and Geothermal Resources Division, Korea Institute of Geoscience and Mineral Resources, Daejon 34132, Republic of Korea

적물을 뚫고 발달하였다. 따라서 대량의 외부수가 천부에서 공급되고 폭발적인 마그마-물 반응을 일으킬 수 있었다. 한 코어의 다이아트림은 역들의 기질지지, 기질 함량의 미약한 수직 변화, 그리고 입자 정착과 관련된 구조의 부재 등 다이아트림 충전물이 극도로 습했거나 물에 포화되어 있었음을 지시하는 특징들을 보여준다. 이 코어에서는 섬세하게 굴곡진 가장자리를 지닌 유동형의 역들이 나타나는데, 이들은 물에 포화되어 매우 유동성이 큰 화산재와 물의 반죽 내에서 역의 마모와 파괴가 거의 일어나지 않았음을 지시한다. 이 화산재와 물의 반죽은 수증기마그마성 다이아트림 및 킴벌라이트형 다이아트림과는 구별되는 얇은 사발 모양의 다이아트림을 채우고 있었다. 다른 코어의 다이아트림 층들은 현무암질 유리질 화산회 기질과 각형의 역들로 이루어져 있으며, 이들은 좀 더 깊은 심도에서 일어난 수증기마그마성 폭발을 지시한다. 이 코어들 중 하나는 화쇄난류에 의해 퇴적된 층상 응회암의 붕괴층을 포함하고 있는데, 이는 이 다이아트림이 수면 위에 만들어진 응회환과 관련이 있었음을 지시한다. 따라서 섯치형 분화와 수증기마그마성 분화가 변동하는 제4기 해수면의 영향 하에 대륙붕에서 일어났던 것으로 해석된다. 제주 지하의 다이아트림들은 마르는 물론 응회환과 응회구를 포함한 모든 수성화산의 분화구 하부에 다양한 크기, 형태, 물성의 다이아트림이 나타날 수 있음을 보여준다.

Introduction

A diatreme is a conically shaped, tephra-filled volcanic structure beneath the crater of a volcanic edifice, most of which are inferred to be produced by phreatomagmatic eruptions (Lorenz et al. 1970, 2016; Lorenz 1986, 2003; White and Ross 2011; Valentine and White 2012). A complicated set of processes operate to form the diatreme structures and infilling deposits, such as explosive interactions of magma and water or wet sediments, excavation and disturbance of the substrate, forceful upward injection of tephra and gas followed by falling back of debris, collapse of wall rocks and volcanic edifices on the surface, and convective mixing of the materials associated with these processes (Lorenz 1986, 2003; White 1991b; Ross and White 2006; Lorenz and Kurszlaukis 2007; White and Ross 2011; Gernon et al. 2013; Ross et al. 2013). Understanding the processes of diatreme formation and deposit emplacement is important not only for unraveling magma-water interactions and related eruption processes but also for mineral exploration (Leckie et al. 1997; Stiefenhofer and Farrow 2004; Zonneveld et al. 2004; Brown et al. 2008b) and analysis of volcaniclastic-filled sedimentary basins (Kwon and Sohn 2008; Son et al. 2012; Lutz et al. 2013).

Although phreatomagmatic eruptions are one of the most common volcanic phenomena on Earth, and many of them are presumed to form diatremes (Fisher and Schmincke 1984; Cas and Wright 1987; Vespermann and Schmincke 2000; Lorenz et al. 2016), case studies of diatremes are greatly outnumbered by those of surficial tephra rings or cones (White and Ross 2011). In addition, non-kimberlite diatremes have been only rarely explored by drilling (Elliott et al. 2015; Jones et al. 2017; Bolós et al. 2021), although they remain mostly in the subsurface. For kimberlite diatremes, conflicting models remain active in spite of decades of research on open pit and underground mines and cores (e.g., Clement 1982; Stiefenhofer and Farrow 2004; Sparks et al. 2007; Wilson and Head 2007a; Wilson and Head 2007b; Cas et al. 2008; Brown et al. 2008a; Porritt et al. 2008a, b; Brown et al. 2009; White and Ross 2011; Kjarsgaard et al. 2022).

Jeju Island, Korea, is a large basaltic shield volcano situated on the ca. 100-m-deep continental shelf of the southeastern Yellow Sea (Fig. 1a). Extensive borehole drilling since the 1960s reveals that the shield-forming lavas on the surface of the island are underlain by about 100 m of hydrovolcanic deposits, which consist of primary volcaniclastic deposits formed in tuff rings and tuff cones and secondary volcaniclastic deposits that were resedimented in either subaerial or submarine environments (Sohn and Park 2004; Sohn et al. 2008; Jeon et al. 2013). These deposits are interpreted to have resulted from either Surtseyan or other phreatomagmatic activity on the Yellow Sea continental shelf under the fluctuating Quaternary sea levels over a million years before the effusion of the shield-forming lavas on the surface (Sohn et al. 2008).

In this paper, we describe three selected cores from Jeju Island, which contain previously undescribed hydrovolcanic deposits that are tens of meters thick and massive. Such thick-bedded and massive deposits are not found in any of the rim beds of the hydromagmatic volcanoes on the surface and are not known to have been generated by Surtseyan to phreatomagmatic or maar-forming eruptions (White and Ross 2011). They are therefore inferred to have accumulated in local topographic depressions, more than tens of meters deep, i.e., in the craters or diatremes of tuff rings, tuff cones, or maars. We presume that these cores fortuitously penetrated the diatremes of subsurface volcanoes, providing a rare opportunity to observe the features of diatreme fills and crater-filling sediments of hydromagmatic volcanoes. This paper describes and interprets the deposit features of the diatreme- and crater-filling sediments of the subsurface hydromagmatic volcanoes and discusses the controls of the fluctuating Quaternary sea levels on the nature of hydrovolcanic activity on a continental shelf.

Geological setting

Jeju Island is a Quaternary volcanic field situated on the ca. 100-m-deep Yellow Sea continental shelf off the Korean Peninsula (Fig. 1a), where tidal currents are one of the most

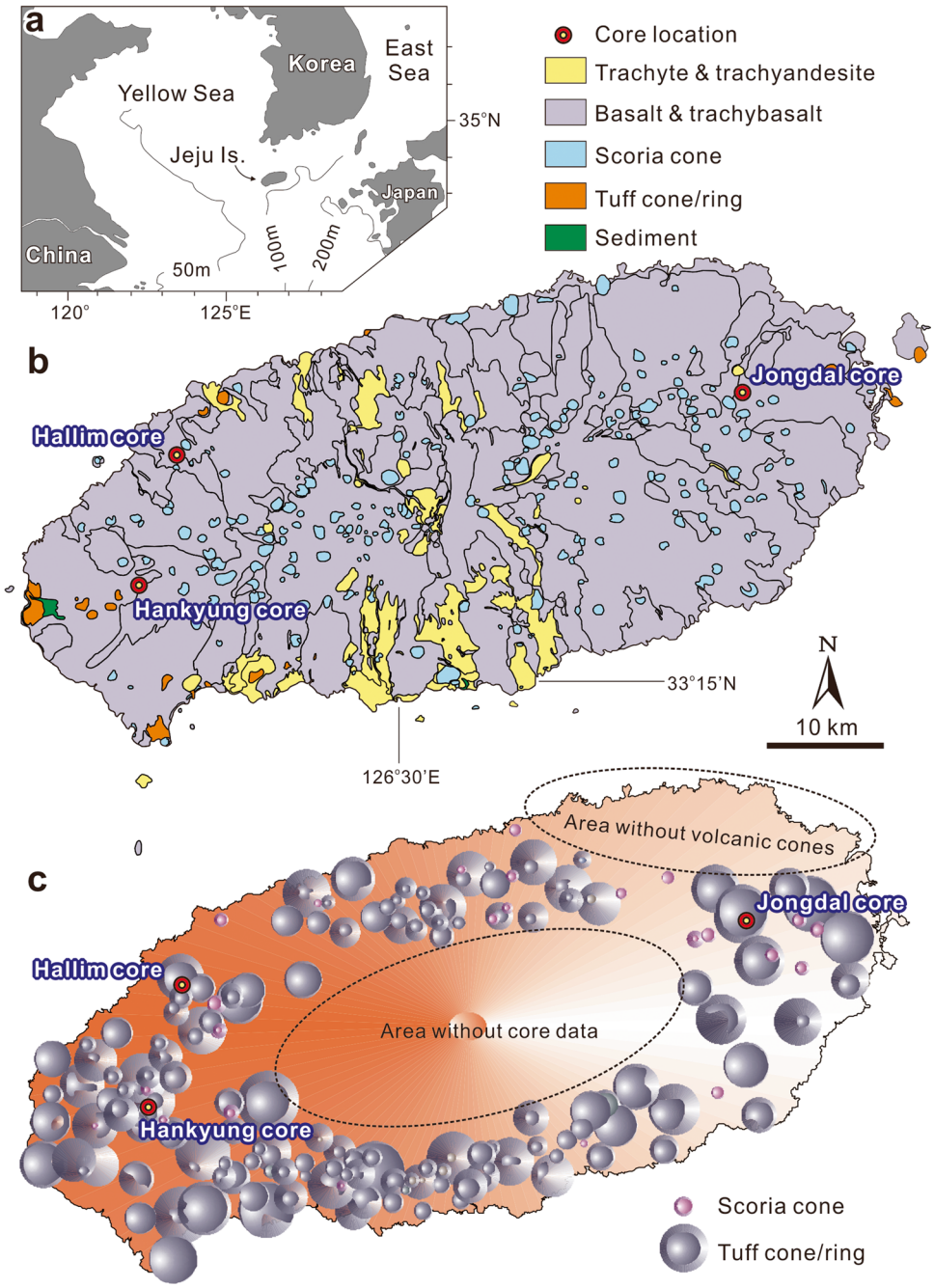

Fig. 1 Location and geology of the study area. **a** Jeju Island is an intraplate volcano situated on the ca. 100-m-deep continental shelf of the Yellow Sea. **b** Geologic map of Jeju Island with the locations of the studied cores (simplified after Park et al. 2000). **c** Distribution of subsurface volcanic cones beneath the shield-forming lavas in Jeju Island based on the compilation of core data from ca. 1400 boreholes. The diameter of individual volcanic cones was determined based on the correlation of multiple cores adjacent to each other, which are several tens to a few hundreds of meters apart. The circles, therefore, reflect the actual edifice size of the subsurface volcanoes, although the accuracy of correlation of the subsurface volcanic cones, which are commonly less than a few kilometers in diameter, cannot but be low when the cores are more than a few hundred meters away from each other. The volcanic edifice type (tuff ring, tuff cone, or scoria cone) was interpreted from the lithofacies characteristics of the volcaniclastic deposits (Sohn et al. 2008)

important agents of sediment deposition, erosion, and resuspension. Extensive fields of tidal sand ridges are distributed in places on the shelf, including the Jeju Island area (Liu et al. 1998; Shinn et al. 2007). The island consists of an elliptical shield volcano, ca. 70×30 km^2 in size, 1950 m in height, and dotted with over 300 scoria cones, a few dozens of hydromagmatic volcanoes, and a few lava domes. The lavas have the compositions of mainly alkali basalts to trachytes and subordinately sub-alkali basalts to andesites (Park 1994; Park et al. 1999; Tatsumi et al. 2005). They erupted generally between ca. 1.0 and 0.01 Ma (Koh et al. 2008, 2019; Koh and Park 2010a, b; Yeo et al. 2019). Holocene to historical eruptions are also increasingly reported (Sohn et al. 2015; Marsden et al. 2021). Geochemical and geophysical studies suggest that Jeju Island is neither a hot spot nor a subduction zone or arc volcano but an intraplate volcano that lacks evidence for plume activity and slab metasomatism. The island is interpreted to have resulted

more likely from decompression melting of the upper mantle at the edges of the subducted Pacific and Philippine Sea plates that have been stagnant in the mantle transition zone for millions of years (Brenna et al. 2015; Ward et al. 2021).

Methods and terminology

Borehole drilling has been carried out for over half a century on Jeju Island to develop and monitor groundwater under the supervision of the Water Resources Office of the Jeju Special Self-Governing Province. The boreholes are drilled about 30 cm in diameter to insert a monitoring device. Mesoscopic structures that are observable on ordinary outcrops can thus be observed on the recovered cores. Graphic logging of the cores was made outdoors at the drilling site within days after drilling was completed because it was not possible to transport the huge cores to an indoor storage facility and because the cores are destroyed, lost, or disturbed within days to months. The graphic logging recorded the characteristics of the lavas and volcaniclastic rocks, including sedimentary structure, clast size, shape, composition, color, and vesicularity, matrix grain size, sorting, and inclusion of exotic particles such as shells, woods, and intraformational clasts. Representative core samples were brought to the laboratory and prepared for slabs and thin sections for microscopic observations of the petrographic features. Point counting of clast types and abundance was made for one of the cores using a transparent film with a grid of 10 × 10 cm area drawn at 1 cm intervals on the core.

There is a spectrum of eruption styles that result from explosive interactions of magma and water. One endmember is an eruption that involves explosive interaction of magma with groundwater or wet sediment in the subsurface and produces commonly buoyancy-dominated tephra jets or plumes and pyroclastic currents. The term "phreatomagmatic" is used for such an eruption in this paper, although the term "Taalian" is also used as a synonym (Kokelaar 1986; Sohn 1996). The term "Surtseyan" is used for the other endmember of eruptions, which occur in shallow waters, involve the interaction of magma with a mobile mix or slurry of tephra and surface water filling a shallow funnel-shaped vent, and generate mostly short-lived and inertia-dominated tephra jets (Thorarinsson et al. 1964; Thorarinsson 1967; Kokelaar 1983; Moore 1985). We use the terms "hydrovolcanic" and "hydromagmatic" as broad terms that can encompass both phreatomagmatic and Surtseyan eruptions, as have already been used for a long time (Wentworth 1938; Sheridan and Wohletz 1983; Wohletz and Sheridan 1983; Wohletz and McQueen 1984; Németh and Kósik 2020). For example, we use the term "hydromagmatic volcano" when collectively referring to all different types of volcanoes produced by "hydrovolcanic activity" or "hydrovolcanism," such as tuff rings, tuff cones, and maars.

We use the terms "tuff ring," "tephra ring," and "ejecta ring" synonymously, irrespective of whether the "ring" surrounds a crater excavated below the pre-eruption surface or not and whether the ring is composed of "tuff" or coarser-grained deposits. Some researchers seem to avoid the use of the term "tuff ring" when describing the volcaniclastic deposits around a maar crater, and instead use the terms "tephra ring" or "ejecta ring" probably because of the belief that "tuff rings" and "maars" are distinctly different volcanoes and the term "tuff ring" is inadequate to describe the volcaniclastic deposits around the crater of a "maar." As has already been argued in another paper (Sohn et al. 2021), tuff rings and maars, or maar-diatreme volcanoes, belong to the same category of volcanoes, and the term "tuff ring" can be used to describe the "tephra ring" or "ejecta ring" of a maar.

Subsurface stratigraphy and lithology

The shield-forming lavas of Jeju Island are underlain by basaltic volcaniclastic deposits named the Seoguipo Formation (Koh 1997). Deposition of the formation began at ~ 1.88 Ma and continued until ~ 0.5 Ma (Koh et al. 2013, 2017a, b, 2022). The formation has an average thickness of 100 m and occurs throughout the island in the subsurface except in the northeastern margin. The formation is composed mainly of overlapping rim beds of tuff rings and cones with intercalations of volcaniclastic to epiclastic, subaerial to submarine, and rarely fossiliferous deposits that accumulated under the influence of fluctuating sea levels during the Early Pleistocene (Sohn and Park 2004; Sohn et al. 2008). More than a hundred volcanic cones were identified in the formation by compiling the core data from about 1400 boreholes (unpublished data of K.H. Park) (Fig. 1c). The upper surface of the formation is highly rugged because of the protrusion of these volcanic cones. A few of them are only partly buried by the later lava flows and exposed to the surface (Sohn and Park 2005).

The Seoguipo Formation is underlain by a still poorly consolidated and unlithified sedimentary deposit named the U Formation (Koh 1997). The formation has variable thicknesses between 70 and 250 m and is composed of moderately to well-sorted quartzose sand and mud that are devoid of volcanic particles but contain rare mollusk shell fragments (Jeong et al. 2016). Calcareous nannofossils and diatoms in these sediments suggest that the formation was deposited from the Pliocene to the earliest Pleistocene (Yoon et al. 2004). The formation is therefore interpreted to be deposits of the tidal sand ridges and inter-ridge fines that accumulated on the continental shelf before the onset of volcanism in the Jeju Island area (Koh

1997; Sohn and Park 2004). Although temporally unrelated to Jeju volcanism, the formation played an important role in modulating the eruption and growth of the overlying hydromagmatic volcanoes by acting as a "soft" substrate (Sohn and Park 2005) and as a source of the "dirty" coolant for the hydroexplosions (Sohn 1996; White 1996b; Schipper et al. 2011).

The basement rocks beneath the U Formation are composed of Jurassic and Cretaceous granites in the majority of the island (Kim et al. 2002), Cretaceous to Paleogene volcanic rocks (andesitic to rhyolitic lavas and tuffs) in the eastern margin of the island, and quartzose metasedimentary rocks of unknown age in the southwestern part of the island (Go et al. 2017). These rocks occur 155 to 312 m (ca. 250 m on average) below sea level.

General characteristics of cores

In this paper, we describe three selected cores, which contain tens-of-meter-thick intervals of massive deposits (Fig. 2). The Hallim core (Fig. 3a) was obtained from a site at an altitude of 57 m above sea level in the northwestern part of Jeju Island (Fig. 1b). The 107-m-thick upper portion of the core consists of a succession of meter-thick aa lavas and decimeter- to meter-thick pahoehoe lavas with interlayers of clinker and paleosol (or sedimentary deposits that have undergone pedogenic alteration) (Fig. 2a). The lowermost lava unit has a glassy rim at the base and is underlain by black sand and granule (Fig. 3b), composed of non-vesicular and angular sideromelane or tachylite particles that are interpreted to be hyaloclastite (Fig. 3c). The Seoguipo Formation is 55 m thick (core depth: 125–180 m) and occurs 68 m below sea level. The U Formation occurs 125 m below the sea level (core depth: > 182 m) and is composed of moderately to well-sorted, quartzose fine sand (Fig. 3d). The contact between the Seoguipo and U Formations is transitional over 2 m (core depth: 180–182 m) and characterized by chaotic mixing of basalt and mudstone clasts and well-sorted quartzose sand (Fig. 3e).

The Hankyung core (Fig. 4a) was obtained from a site at an altitude of 140 m above sea level in the western part of Jeju Island (Fig. 1b). The upper 187-m-thick portion of the core consists of meter- to decameter-thick aa and

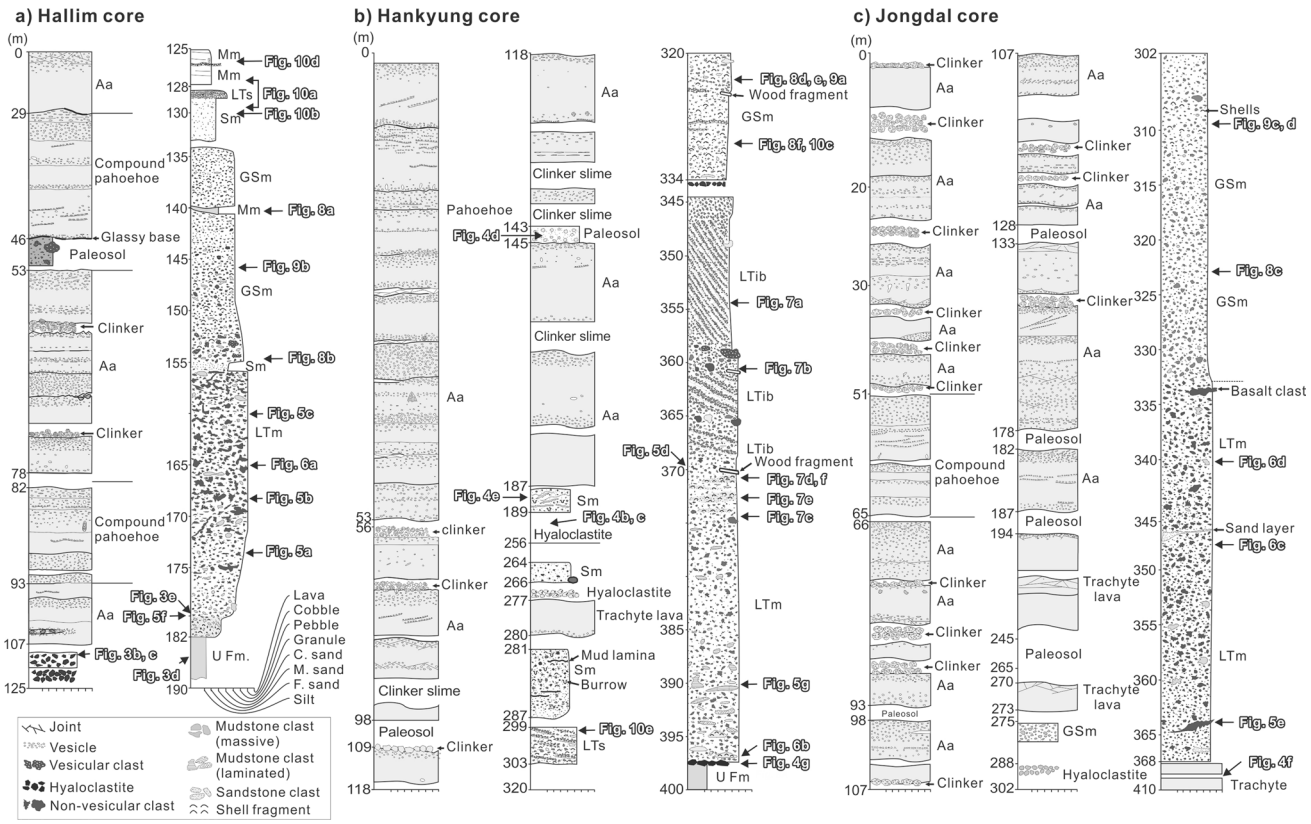

Fig. 2 Graphic columns of the three cores analyzed for this study. **a** Hallim core. The elevation of the core site is 57 m a.s.l. GPS coordinates of the site are 33° 24′ 26.4″ N and 126° 17′ 53.5″ E. **b** Hankyung core. The elevation of the core site is 140 m a.s.l. GPS coordinates of the site are 33° 19′ 08.42″ N and 126° 16′ 22.09″ E. **c** Jongdal core. The elevation of the core site is 198 m a.s.l. GPS coordinates of the site are 33° 16′ 07.9″ N and 126° 18′ 06.8″ E (see Fig. 1 for the locations of the cores)

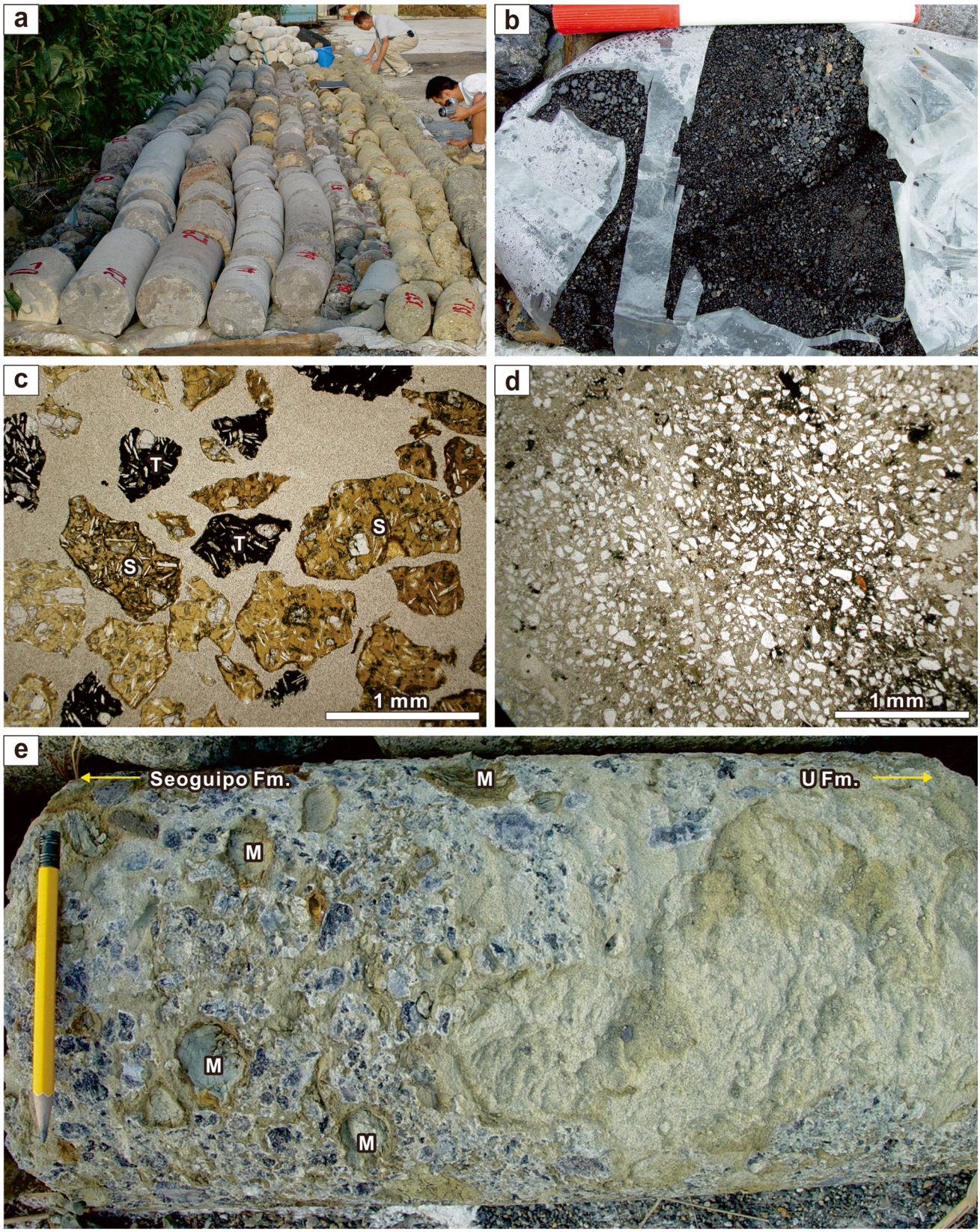
a
b
c
T
T
S
S
1 mm
d
1 mm
e
Seoguipo Fm.
M
U Fm.
M
M
M

◂**Fig. 3** General features of the Hallim core. **a** A view of the Hallim core. **b** Black basaltic sand and granule interpreted to be hyaloclastite (depth: 109 m). **c** Thin-section photomicrograph of the hyaloclastite shown in **b**, composed of non-vesicular and angular sideromelane (S) and tachylite (T) particles. **d** Thin-section photomicrograph of the quartzose fine sand from the U Formation (depth: 185 m). **e** Transitional contact between the Seoguipo Formation and the underlying U Formation, composed of both basalt and mudstone (M) clasts in a well-sorted fine sand matrix (depth: 180 m). The pencil for scale is 12 cm long

pahoehoe lavas with rare intercalations of clinker and paleosol (Fig. 4d). Core recovery was poor between the 187- and 277-m interval above a 3-m-thick trachytic lava (Fig. 2b). Black basaltic glassy sand and granule (hyaloclastite) (Fig. 4b, c), massive mudstone with chaotically deformed basaltic sandy interbeds (Fig. 4e), and massive sand deposits were recovered from this interval with uncertain stratigraphic relationships between them (Fig. 2b). A succession of 118-m-thick basaltic volcaniclastic deposits occurs to a depth of 397 m (257 m below sea level). The U Formation at the base of the core is composed of massive and poorly consolidated mud. Partly glassy basalt clasts, inferred to be hyaloclastite or pillow fragment breccia, are intercalated between the Seoguipo and U Formations (Fig. 4g).

The Jongdal core was obtained from a site at an altitude of 198 m above sea level in the eastern part of Jeju Island (Fig. 1b). The lavas here are 273 m thick and consist of meter- to decameter-thick aa and pahoehoe lavas and intervening clinker and paleosol layers (Fig. 2c). The Seoguipo Formation is 93 m thick (core depth: 275 – 368 m; 77 to 170 m below sea level) and underlain by trachytic lava and hyaloclastite (Fig. 4f). The U Formation is not found at this site probably because the core did not reach the formation.

Lithofacies characteristics of the Seoguipo Formation

Three major lithofacies constitute the Seoguipo Formation of the studied cores: (1) massive, generally matrix-supported basaltic lapilli tuff (facies LTm), (2) steeply inclined-bedded deposit of crudely to thinly stratified lapilli tuff and tuff and massive to crudely stratified gravelly sandstone (facies LTib), and (3) massive, generally matrix-supported, volcaniclastic gravelly sandstone (facies GSm). Other volumetrically minor facies includes massive volcaniclastic sandstone (facies Sm), crudely stratified volcaniclastic sandstone (facies Ss), and massive mudstone (facies Mm). Individual cores show overall similar vertical facies changes from massive lapilli tuff (facies LTm) at the base through massive gravelly sandstone (facies GSm) in the middle to finer-grained and thinner-bedded deposits (facies Ss, Sm, and Mm) at the top (Fig. 2). Steeply inclined-bedded deposit (facies LTib) occurs only in the Hankyung core between the massive lapilli tuff and the massive gravelly sandstone facies.

Massive lapilli tuff (facies LTm)

Description

Massive lapilli tuff is 26 m thick in the Hallim core (depth: 156 – 182 m; Fig. 2a), 22 m thick in the Hankyung core (depth: 375 – 397 m; Fig. 2b), and 35 m thick in the Jongdal core (depth: 333 – 368 m; Fig. 2c). It consists of basalt and sedimentary rock (mostly mudstone) fragments supported in a poorly sorted and detrital quartz-rich sideromelane ash matrix (Fig. 5). Basement-derived accidental lithic clasts are not identified in all cores. The basalt clasts are mostly aphyric, fine-to-medium lapilli-sized, and rarely coarse lapilli- to block-sized (grain size terms after White and Houghton 2006). In the Hallim core, the basalt clasts are generally glassy and poorly to moderately vesicular and have irregular shapes of rag, amoeboid, and disk with uneven margins (Fig. 5a, b). Scoriaceous bomb-like clasts with finely vesicular margins and coarsely vesicular interior are also common (Fig. 5c). In the Hankyung and Jongdal cores, the basalt clasts are non-vesicular and mostly angular and blocky in shape (Fig. 5d), although some block-sized clasts in the Jongdal core have partly irregular or fluidally shaped margins (Fig. 5e).

Sedimentary clasts are composed mainly of mudstone and rarely of sandstone (Fig. 5f, g). Mudstone fragments are fine lapilli- to block-sized, angular to subrounded and irregular in shape, light gray to light brown in color, and internally massive or crudely laminated (Fig. 5g). Some of them contain abundant shell fragments. On the other hand, sandstone clasts have irregular or contorted shapes and diffuse and disseminated margins (Fig. 5f) and are found only rarely in the lower part of the facies unit.

Point counting of clast types and their abundance in the Hallim core shows that the core does not show meaningful changes in clast type or abundance through the facies unit except for the abundance of sedimentary clasts and shell fragments near the base of the unit (Table 1). Microscopic observations show that the matrix consists predominantly of non- to poorly vesicular sideromelane shards and subordinately of opaque tachylite particles (Fig. 6). The sideromelane particles have generally round and undeformed vesicles and fluidally shaped (Fig. 6a) to curviplanar or subrounded margins (Fig. 6c, d). Detrital quartz grains are ubiquitous. Characteristically green glauconite (glaucony) particles (Odin and Matter 1981; Banerjee et al. 2016) are also common in the quartz-rich matrix (Fig. 6b). Shell fragments are locally abundant near the contact with the U Formation (Fig. 6b).

Fig. 4 General features of the Hankyung and Jongdal cores. **a** A view of the Hankyung core. **b** Black basaltic sand and granule (hyaloclastite) (Hankyung core; depth: 202 m). **c** Thin-section photomicrograph of the hyaloclastite shown in **b**, composed of non-vesicular and angular sideromelane (S) and tachylite (T) particles. **d** Reddish brown and poorly sorted mud containing basalt clasts, interpreted to be a paleosol layer intercalated between two lava flow units (Hankyung core; depth: 144 – 145 m). **e** Massive mudstone with deformed (convoluted) basaltic sandy interbeds (Hankyung core; depth: 188 m). **f** Dark gray glassy particles (left) and trachytic lava (right) at the base of the Jongdal core (depth: 408 m). **g** Massive lapilli tuff at the base of the Seoguipo Formation overlies the massive mudstone of the U Formation in the Hankyung core (depth: 397 – 398 m). Partly glassy basalt clasts between these formations can be hyaloclastite or pillow lava fragments. The pencil for scale is 12 cm long

Interpretation

The angular/blocky to irregular/fluidally shaped basalt clasts in this facies are interpreted to have formed by the mingling of ascending vesiculating to non-vesiculated magma and wet and unconsolidated, and probably liquefied sediment of the U Formation (Kokelaar 1982; Hanson and Wilson 1993; Zimanowski and Buttner 2002). The coarse mixing

of magma and sediment was probably followed immediately by either brittle fragmentation or ductile tearing apart of magma, similar to the blocky to fluidal peperite-forming processes (Busby-Spera and White 1987; Hanson and Hargrove 1999; Lorenz et al. 2002; McClintock and White 2006; Martin and Németh 2007; McClintock et al. 2008; Befus et al. 2009), fuel–coolant interactions, and explosive expansion of steam or vapor and dispersion of tephra (Zimanowski et al. 1997, 2015; Zimanowski 2001). The complete absence of bedding in the lapilli tuffs, except for a possible sandy interbed in the Jongdal core (depth: 346 m; Fig. 2c), which may be a sedimentary clast larger than the core diameter, suggests that the lapilli tuffs represent an unsorted mixture of the diatreme-filling slurry. Crude stratification or bedding is expected to be found if the lapilli tuffs were emplaced by multiple pyroclastic fall or density current events on the syneruptive crater floor without later disruption (Stiefenhofer and Farrow 2004; Ross and White 2005; Lorenz 2008; Moss et al. 2008; White and Ross 2011; Elliott et al. 2015; Lorenz et al. 2016).

The preservation of ragged to discoid clast shapes and delicate reentrant margins in the Hallim core (Fig. 5a – c) suggests that the basalt clasts experienced minimal abrasion and breakage associated with granular mixing in the diatreme after initial magma fragmentation. The preservation of contorted sedimentary clasts with diffuse and disseminated margins (Fig. 5f) and local concentration of shells and sedimentary clasts (Table 1) also suggests incomplete mixing and homogenization of the diatreme-filling debris in addition to negligible particle abrasion and breakage in the diatreme. We, therefore, infer that the Hallim core penetrated the "dead zone" in the diatreme margins, where the materials were unaffected by the violent diatreme processes, such as debris or gas jetting from below or falling back of debris that was explosively ejected by explosions (White and Ross 2011).

We infer that the diatreme-filling materials had the properties of a mobile slurry and contained abundant water-rich or water-saturated matrix. The slurry might have been cohesive if a sufficient amount of mud, which consists of illite, kaolinite, smectite, and chlorite (Jeong et al. 2016), was introduced into the slurry from the U Formation. The lack of clast-supported to openwork texture in the lapilli tuff suggests that the fine-grained materials in the diatreme could not be efficiently winnowed by, e.g., upward-directed debris jets or gas jets. Meager vertical changes in the proportion of the matrix (Table 1) are also interpreted as evidence against the role of gas or steam fluidization in the diatreme. The absence of ash aggregates or ash-coated particles (Fig. 6a) suggests that the diatreme fill was water-saturated, and particle adhesion was inhibited because of the lack of surface tension effects in water-saturated slurry (Go et al. 2017). We, therefore, infer that the diatreme-filling materials could be locally injected upward by gas- and steam-propelled jets of debris near the loci of explosions, but these jets could not elutriate the fine-grained materials in the other part of the diatreme because these materials were wet or even water-saturated.

Vigorous mixing and particle abrasion of the diatreme-filling materials are not inferred to have occurred in the diatremes of the Hankyung and Jongdal cores because the clasts in these cores also preserve sharp corners and irregular protrusions along their margins (Fig. 5d, e). Even fragile mudstone clasts appear to have been subject to negligible abrasion and breakage in the Hankyung core (Fig. 5g). The absence of features related to ash aggregation (Fig. 6b – d) can also be the result of water saturation of the diatreme fills in these cores.

Steeply inclined-bedded deposit (facies LTib)

Description

A 24-m-thick interval of unusually steeply dipping (50° to 80°) tuff (Fig. 7a) and gravelly sandstone (Fig. 7b) occurs in the middle of the Seoguipo Formation in the Hankyung core (depth 345 – 369 m, Fig. 2b). The steeply inclined-bedded deposits within this interval are defined as an independent facies, irrespective of the constituent facies, which consist of (1) thin-bedded tuff characterized by alternations of centimeter-thick, variably graded, very fine to coarse ash layers with subtle thickness variations (Fig. 7a), (2) crudely stratified gravelly sandstone (Fig. 7b), and (3) massive gravelly sandstone (Fig. 7d). The gravelly sandstones contain mostly crystalline and heteromictic, rarely rounded basalt clasts (Fig. 7b, d). A wood fragment is also found in this deposit (Fig. 7b). About a 4-m-thick interval (core depth: 369 – 373.5 m) between this facies and the underlying massive lapilli tuff (facies LTm) is composed of massive mudstone intercalated with mollusk shell-bearing sandstone layers (Fig. 7c, e) and containing a wood fragment (Fig. 7f).

Interpretation

The meter-thick interval of wood-bearing mudstone and shell-bearing sandstone between this facies and the underlying massive lapilli tuff (Fig. 7c, e, f) indicates that this facies formed after the volcanic eruption ended. The unusually steep bedding in this facies, which far exceeds the angle of repose, is interpreted to be due to neither tectonic tilting nor the artificial effect of borehole drilling but to be the result of penetration of the borehole into steeply dipping deposits of primary tuffs and reworked volcaniclastic deposits. Steep bedding here is also not attributed to subsidence

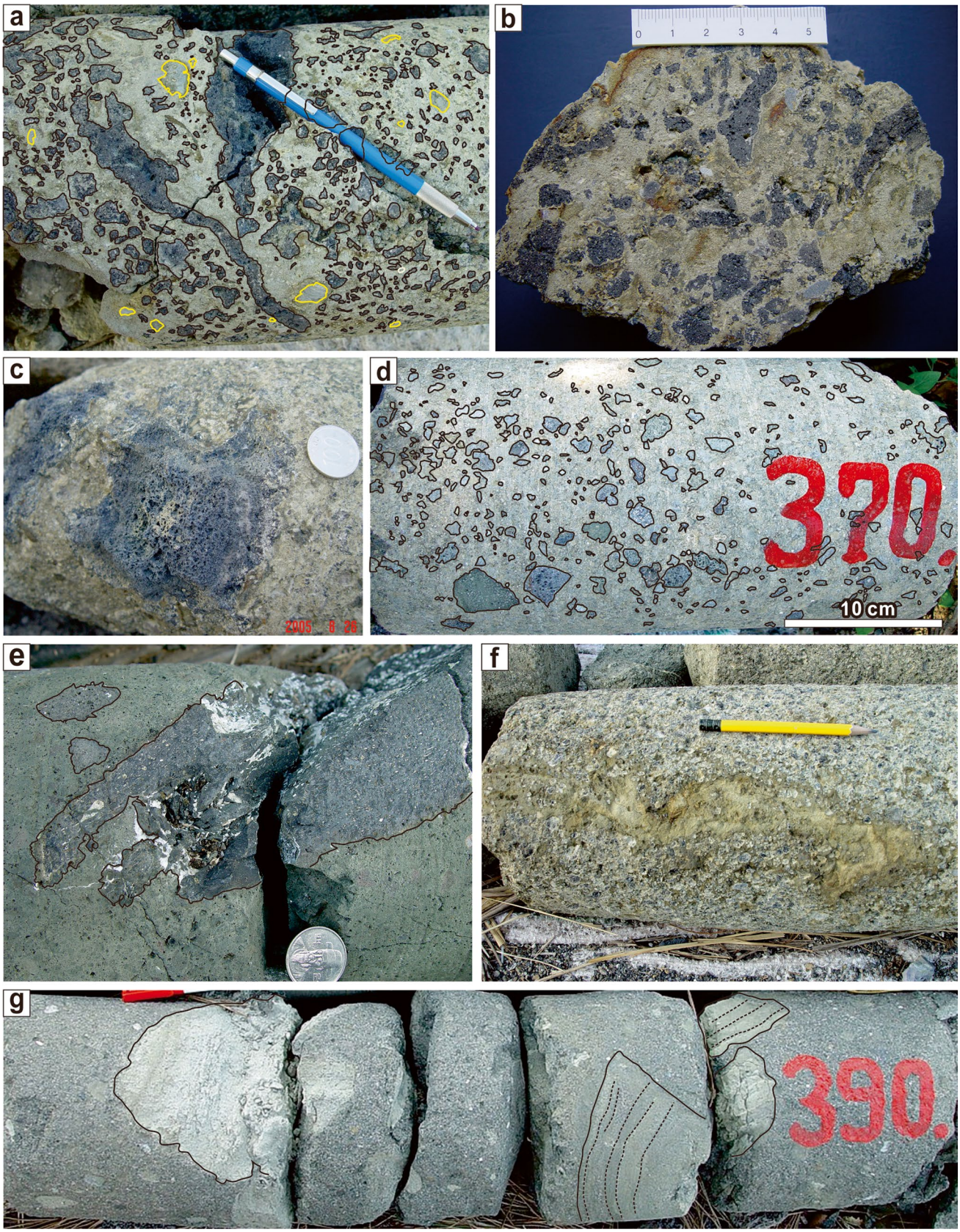
a
b
0 1 2 3 4 5
c
2005 8 26
d
370
10 cm
e
f
g
390

◂**Fig. 5** Clasts of massive lapilli tuff (facies LTm). **a** Irregular to ragged and vesicular basalt clasts and mudstone clasts (outlined by yellow line) set in a detrital quartz sand-rich ash matrix from the Hallim core (depth: 174 m). The pencil for scale is 15 cm long. **b** Irregular and vesicular basalt clasts in a detrital quartz sand-rich matrix from the Hallim core (depth: 168 m). **c** Scoriaceous bomb-like clasts from the Hallim core (depth: 160 m) having irregular and poorer vesicular margins and a highly vesicular interior. **d** Generally blocky and non-vesicular basalt clasts from the Hankyung core (depth: 370 m). **e** Non-vesicular and irregularly shaped basalt clasts from the Jongdal core (depth: 364 m). The matrix is composed of massive lapilli tuff, in which basaltic lapilli are non-vesicular and have blocky and equant shapes. **f** Massive lapilli tuff of the Hallim core, containing an elongated and contorted sand fragment with diffuse margins (depth: 180 m). The pencil for scale is 12 cm long. **g** Massive lapilli tuff containing large, massive, or laminated mudstone fragments near the base of the Hankyung core (depth: 390 m). The coin in **c** and **e** is 2.4 cm in diameter

of syn-eruptive bedded upper diatreme deposits (Suhr et al. 2006; Lorenz 2008; White and Ross 2011; Delpit et al. 2014; Lorenz et al. 2016) because this facies is post-eruptive. The steep bedding in this facies is therefore attributed to the failure of the tephra beds and overlying sediments that accumulated on the surface around the volcano. A few alternations of steeply inclined-bedded and massive deposits (Fig. 2b) suggest that the failure occurred in multiple mass movement events involving rockfall or rock slide of semi-consolidated materials with minimal internal deformation and debris flow of remolded materials. The wood fragments (Fig. 7b, f) suggest that the failure occurred after vegetation development on the surface years after the cessation of the eruption. Vegetation development on the surface of the volcano at the time of eruption, which commonly lasts only days to months (Simkin and Siebert 1984, 2000), seems unlikely.

Massive gravelly sandstone (facies GSm)

Description

The massive gravelly sandstone facies is 22 m thick in the Hallim core (depth: 134 – 155 m; Fig. 2a), 14 m thick in the Hankyung core (depth: 320 – 334 m; Fig. 2b), and 31 m thick in the Jongdal core (depth: 302 – 333 m; Fig. 2c). It is not clear how many depositional units constitute the massive deposits, but the presence of a mudstone interbed (or a mudstone clast larger than the core diameter) in the Hallim core (Fig. 8a), non-uniform distribution of clast types and shell fragments, and vertical alternations of clast-supported to matrix-supported textures suggest that the massive deposits consist of multiple, meter-thick, amalgamated units that have subtly different clast types and contents. The basalt clasts in this facies are either matrix- or clast-supported and show diverse colors, vesicularity, crystallinity, and angularity in the Hallim and Jongdal cores (Fig. 8b, c). However, the massive deposits of the Hankyung core comprise matrix-supported sideromelane lapilli and rare mudstone (or extremely fine-grained tuff) fragments in a sideromelane ash matrix (Fig. 8d). A lapilli tuff clast (Fig. 8e), deformed "ghost" bedding (Fig. 8f), and wood fragments (Fig. 2b) are also found in this core. Shell fragments are found in all cores, either sparsely scattered in the massive deposits or forming indistinct layers or lenses. Under the microscope, the matrix consists predominantly of yellowish to brownish sideromelane and relatively rare opaque tachylite particles (Fig. 9). Rounded or abraded particles are more commonly found here than in the matrix of the massive lapilli tuff.

A meter-thick massive sandstone (facies Sm) is intercalated between this facies and the underlying massive lapilli tuff (facies LTm) in the Hallim core (depth 155 m; Fig. 2a). A hyaloclastite layer (poorly retrieved as core) lies between this facies and the underlying steeply inclined-bedded deposit (facies LTib) in the Hankyung core (depth 334 – 345 m; Fig. 2b). The contact with the underlying massive lapilli tuff is indistinct and gradational in the Jongdal core (depth: 333 m; Fig. 2c).

Interpretation

The massive and matrix- or clast-supported gravelly deposits are interpreted to have been deposited by either cohesive or friction-dominated debris flows (Nemec and Steel 1984; Shultz 1984; Blair and McPherson 1998; Sohn et al. 1999; Sohn 2000). The diversity of clast types (Fig. 8b), rounding of some clasts (Fig. 8c), and the inclusion of friable mud (or extremely fine-grained tuff) or lapilli tuff clasts (Fig. 8d, e) suggest that the materials for these debris flows originated from diverse sources, including primary volcaniclastic deposits surrounding the crater of a tuff ring/cone and fluvially or wave-reworked volcaniclastic deposits in a volcaniclastic apron around a volcano (Busby-Spera 1988; Karatson and Németh 2001; Allen et al. 2007; Casalbore et al. 2010). Particle rounding in the matrix is not always evident (Fig. 9), probably because of the short transport distance and insignificant reworking of tephra at the depositional site.

The emplacement setting of the debris flows is interpreted to have been subaqueous based on the intercalation of a mud layer (or a mudstone clast wider than the core diameter) in the Hallim core (Fig. 8a), the occurrence of hyaloclastite breccias beneath and above the facies units (Fig. 2), and the upward facies transition into submarine facies (Sm, Ss, and Mm; see below) (Fig. 2). The absence of steep-sided erosion surfaces incised by rill flows or overland flows is also indirect evidence for subaqueous deposition of the deposits (Sohn et al. 2008). The sparse distribution of shell fragments cannot be the evidence for subaqueous deposition because the shell fragments could have been derived from the U Formation and later incorporated into this facies during the remobilization of volcaniclasts. However, shell-bearing

Table 1 Vertical variations of clast type and abundance (in vol. %) in the Hallim core measured by point counting on the core surface using a transparent film with grids of 1 cm apart on the core

Facies code	Core depth	Matrix	Vesicular basalt	Non-vesicular basalt	Mud/sandstone	Shell
GSm	137 – 138 m	57.5	41.5	0	0	1
	138 – 139 m	65	31	0	2	2
	139 – 140 m	69	27.8	0	2	1
	141 – 142 m	67	31	1	1	1
	142 – 143 m	66	34	0	0	0
	143 – 144 m	57.5	42.3	0	0	1
	144 – 146 m	72.8	26.6	0	0	1.5
	146 – 148 m	73.5	26.1	0	1	1
	148 – 150 m	63.7	35.3	1	1	1
	150 – 152 m	61	37	1	1	2
	151.5 m	71.5	26	0	2.5	0
	152 – 154 m	62	25	10	4	0
	154 – 155.5 m	58.3	23.8	13.5	6	0
LTm	156 – 158 m	56.3	42	1	3.5	0
	158 – 160 m	50.3	46.3	3	2	0
	160 – 162 m	57.3	39.3	1	9	0
	162 – 166 m	47	49	2	4	0
	166 – 168 m	46.5	51.5	4	2.5	0
	168 – 170 m	50.3	48.6	0	2.5	0
	170 – 172 m	51.5	47.8	0	1	0
	172 – 174 m	47	48.5	0	6	0
	174 – 176 m	64.3	29.6	1	5.3	0
	176 – 178 m	70	25.7	0	4.3	0
	178 – 180 m	65.7	24	0	11.7	0
	180 – 180.5 m	20	38	0	38	4
	180.5 – 182 m	67	24	0	6	3

lenses or layers are interpreted to indicate a submarine environment.

Other facies

Description

Core recovery was generally very poor above the massive gravelly sandstone facies in all cores (Fig. 2). Our experience suggests that this interval comprised mostly loose and friable deposits of mud, well-sorted sand, and matrix-free gravel or hyaloclastite. The fragmentary cores retrieved from this interval comprise (1) massive or crudely stratified sandstone (facies Sm and Ss) (Fig. 10a – c), (2) massive mudstone (facies Mm) (Fig. 10d), and (3) thinly to crudely stratified lapilli tuff (facies LTs) (Fig. 10a, e). The sandstones are composed of poorly to moderately sorted, fine- to coarse-grained sideromelane sand. Some sandstone layers are rich in mollusk shell fragments (Fig. 10c). The mudstones locally have burrows and commonly deformed sandstone interbeds (Fig. 4e). A stratified basaltic sandstone fragment standing upright is found in the Hallim core (Fig. 10d). The stratified lapilli tuffs show either thin stratification (Fig. 10a) or very crude stratification (Fig. 10e) with either fine ash-rich or fine ash-poor matrix.

Interpretation

The massive or crudely stratified sandstones are interpreted to have been deposited by subaqueous sandy debris flows or concentrated density flows (Mulder and Alexander 2001). Rare intercalations of shell-rich beds (Fig. 10c), common association with massive mudstone facies (Fig. 10d) or hyaloclastite deposits (Fig. 2), and the occurrence of burrows (depth: 282 – 284 m; Hankyung core; Fig. 2b) suggest collectively that these facies were deposited in a subaqueous setting. The massive mudstones also suggest suspension settling of fines in a subaqueous setting. An outsize sandstone clast (Fig. 10d) is interpreted to be rockfall debris from a nearby steep crater wall. The lack of well-developed stratification or cross-stratification is interpreted to be due to the lack of wave and current activity in a wave-protected volcanic embayment or submerged crater. The unusual intercalations of stratified lapilli tuffs are interpreted to have been derived from nearby

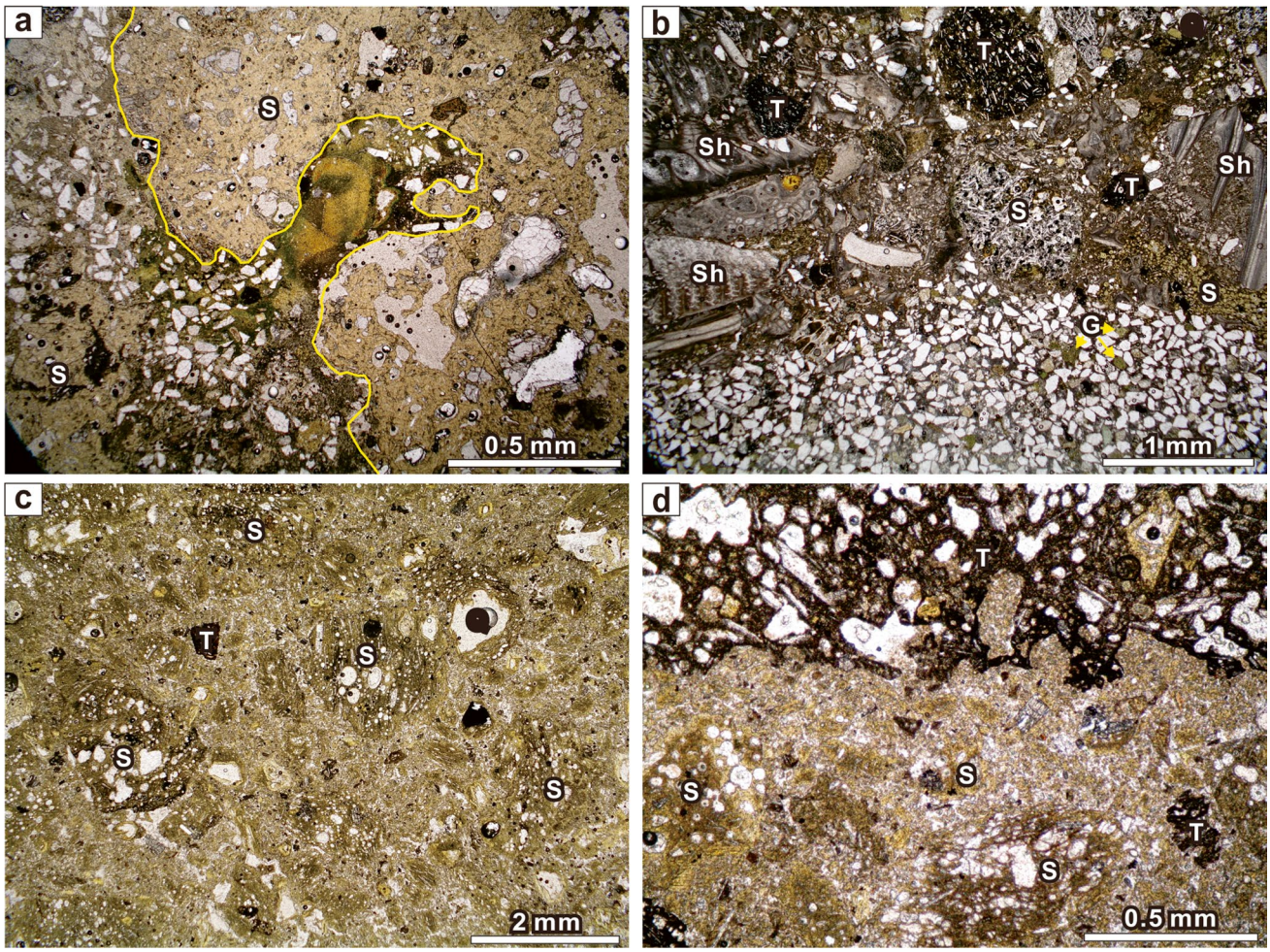

Fig. 6 Photomicrographs of the matrix of massive lapilli tuff (facies LTm). **a** A large non-vesicular sideromelane clast has a fluidally shaped reentrant margin. The matrix in the lower left comprises sideromelane and detrital quartz grains. The specimen is from the Hallim core (depth: 165 m). **b** A specimen from the base of the Seoguipo Formation of the Hankyung core (depth: 397 m) contains abundant shell fragments (Sh) in addition to sideromelane (S) and tachylite (T) particles. Characteristically green particles of glauconite (G), which is a common component of shallow marine sandstone, are abundant in the quartzose matrix. **c** Sideromelane-rich matrix from the Jongdal core (depth: 347 m). The smallest identifiable particles in the interstices are composed of non- to poorly vesicular sideromelane. **d** A tachylite clast in contact with the sideromelane-rich matrix from the Jongdal core (depth: 340 m)

volcanic centers by pyroclastic currents (White 1991a; Moss et al. 2008; Gernon et al. 2009). It is worth noting that these intercalations are found in the Hallim and Hankyung cores, where multiple volcanic cones are interpreted to be superposed or laterally juxtaposed in the subsurface, whereas such intercalation is absent in the Jongdal core where volcanic cones are sparsely distributed (Fig. 1c).

Eruptive and depositional setting in relation to Quaternary sea levels

Jeju Island is regarded as having been subject to negligible crustal motion, either vertical or horizontal, because the Korean Peninsula and the Yellow Sea areas surrounding Jeju Island have remained largely aseismic and tectonically stable compared with other regions in East Asia, such as the Japanese Arc and continental China (Hamdy et al. 2005; Chen 2007; Jin et al. 2007). A rough estimation of the eruptive and depositional setting of the subsurface volcanoes could therefore be made based on the depths of the Seoguipo Formation in the cores in relation to the Quaternary sea levels (Shackleton 1987; Waelbroeck et al. 2002).

The contact between the Seoguipo Formation and the overlying succession of lavas occurs at a depth of 68 m below sea level in the Hallim core, 47 m below sea level in the Hankyung core, and 76 m below sea level in the Jongdal core. The majority of the Seoguipo Formation could therefore have accumulated below sea level except during the glacial maxima (Fig. 11). The facies interpretations given

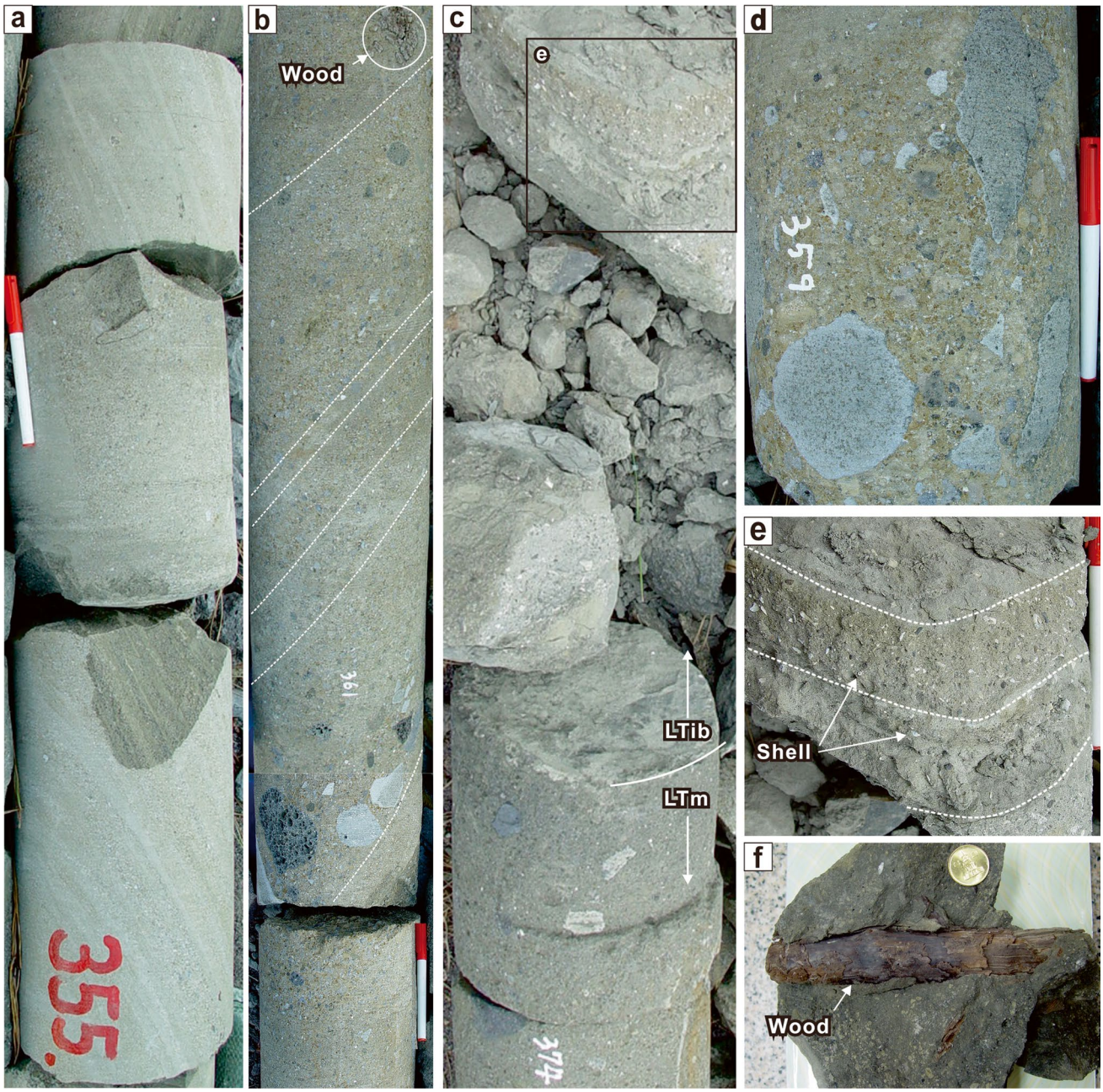

Fig. 7 Features of steeply inclined-bedded deposits (facies LTib) of the Hankyung core. **a** Thinly stratified tuff with very steep bedding (depth: 354 – 355 m). **b** Crudely stratified gravelly sandstone with very steep bedding (depth: 360 – 362 m), containing angular to rounded, crystalline, and heteromictic basalt gravel and a wood fragment. **c** Massive mudstone and interbedded shell-bearing sandstone above the massive lapilli tuff (facies LTm) and beneath the steeply inclined-bedded deposits (depth: 373 – 374 m). **d** Massive gravelly sandstone (facies GSm) containing angular to rounded crystalline basalt gravel (depth: 369 m). **e** Close-up of the shell-bearing sandstone beneath the steeply inclined-bedded deposits (depth: 373 m). **f** A wood fragment in massive mudstone (depth: 370 m). The pen for scale is 12 cm long. The coin in **f** is 2.3 cm in diameter

above and the common intercalations of hyaloclastite near the contact between this formation and the overlying lavas (Fig. 2) support this interpretation.

The level of the contact between the Seoguipo and the U Formations in the cores does not indicate the level of the pre-eruption surface because the contact is more likely the lateral contact between the U Formation and the diatremes that were excavated at least tens of meters to hundreds of meters below the pre-eruption surface. The top surface of the massive lapilli tuff (facies LTm) can, however, provide rough estimates of the upper level of the primary diatreme fill or the level of the syn-eruptive crater floor, which are

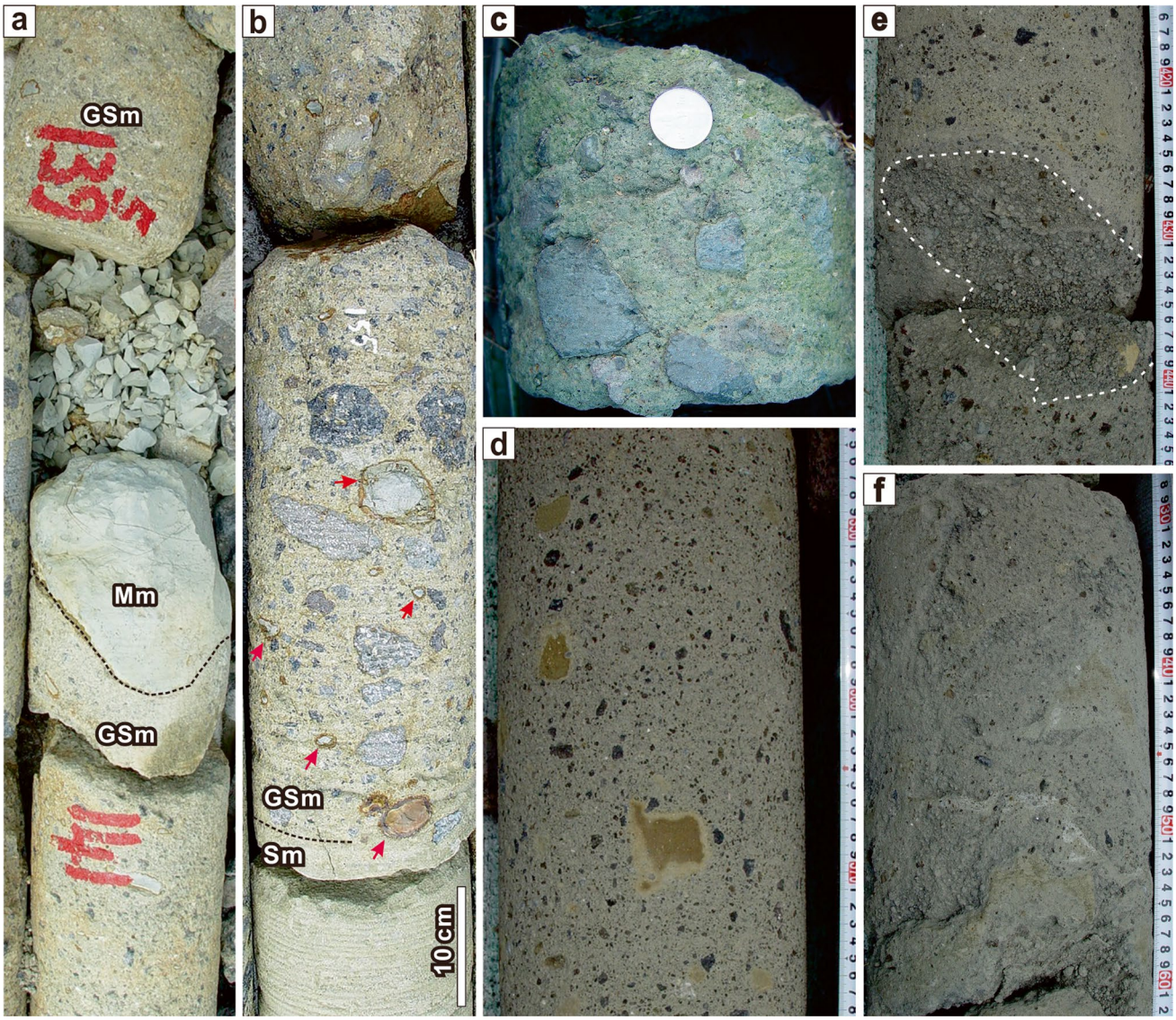

Fig. 8 Features of massive gravelly sandstone (facies GSm). **a** A massive mudstone (facies Mm) is intercalated between massive gravelly sandstone beds (Hallim core; depth: 139 – 141 m). Only part of the mudstone bed is inferred to have been retrieved as a core. **b** A massive gravelly sandstone from the Hallim core (depth: 155 m) consists of a variety of basalt clasts, which vary in color and texture, together with mudstone clasts (red arrows). It overlies a meter-thick massive sandstone (facies Sm). **c** Massive gravelly sandstone from the Jongdal core (depth: 323 m), comprising basalt clasts of different colors and textures. **d** Massive and matrix-supported gravelly sandstone from the Hankyung core (depth: 323 m), containing sideromelane lapilli and irregularly shaped mudstone (or extremely fine tuff) clasts in a sideromelane ash matrix. **e** A lapilli tuff clast is floating in the middle of a massive gravelly sandstone (Hankyung core; depth: 323 m). **f** A massive gravelly sandstone from the Hankyung core, showing irregularly deformed "ghost" bedding (depth: 330 m)

88 m below sea level in the Hallim core, 229 m below sea level in the Hankyung core, and 135 m below sea level in the Jongdal core. The primary diatreme fills are therefore interpreted to have formed mainly below the fluctuating Quaternary sea levels, even during the glacial maxima in the case of the Hankyung and Jongdal cores (Fig. 11). The syn-eruptive crater floors would have thus been flooded with seawater if conditions were met.

No solid evidence is available regarding the diameter, wall angle, and depth of the diatremes. The diatremes are, however, interpreted to belong to volcanic edifices with basal diameters over a few kilometers (Fig. 1c). If these volcanoes are assumed to have had a crater diameter of 1 km and a relatively gentle wall angle near the angle of repose (30°) because of the soft nature of the substrate, the syn-eruptive crater would have had a vertical dimension of ca. 288 m according to simple trigonometric calculations. The crater is therefore inferred to have been rooted about 200 m below the pre-eruption surface or near the contact between the U Formation and the basement if the height of the crater

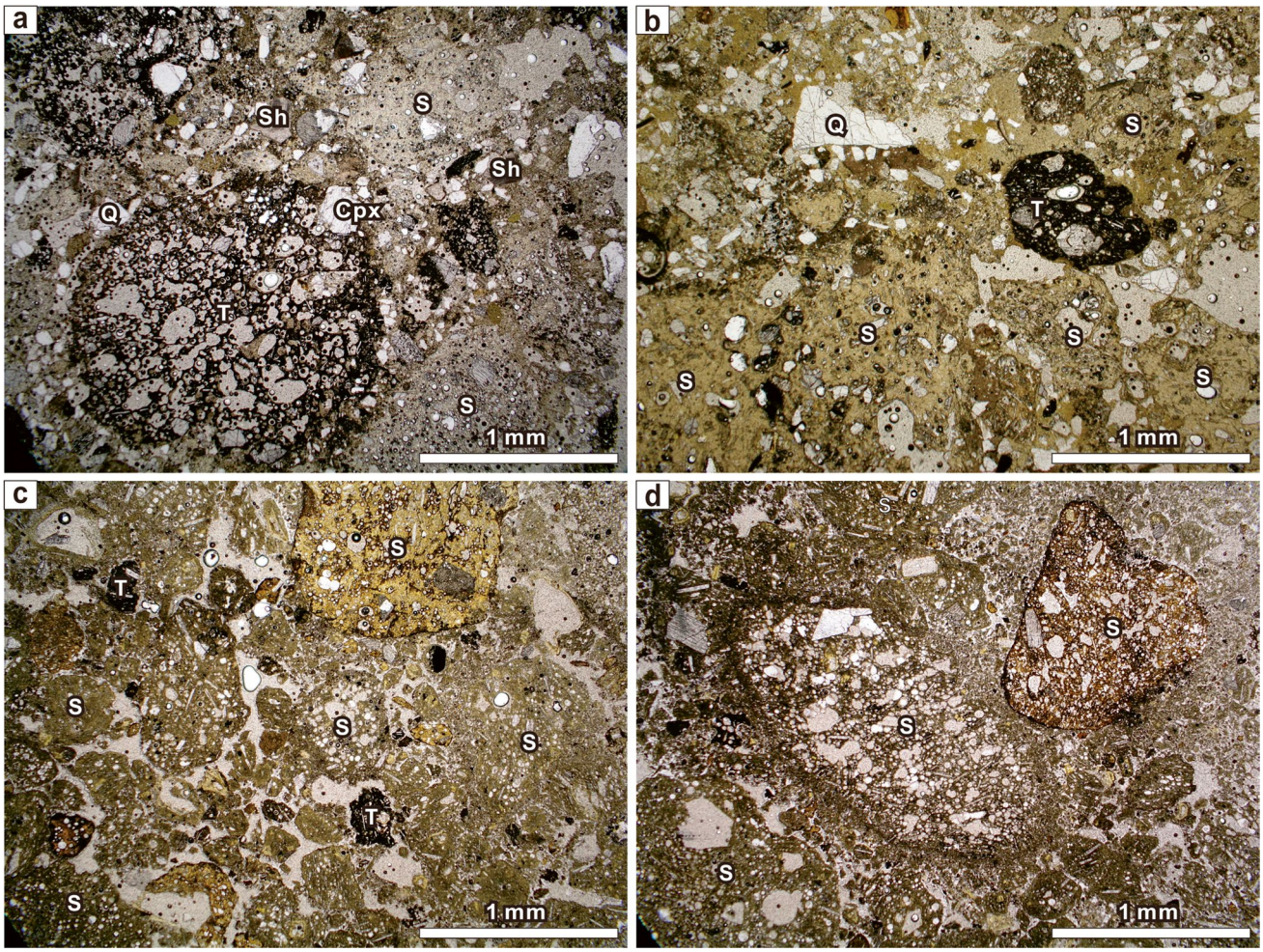

Fig. 9 Photomicrographs of the matrix of massive gravelly sandstone (facies GSm). **a** A specimen from the Hankyung core (depth: 323 m), composed of rounded tachylite particles and finer-grained sideromelane particles. **b** A specimen from the Hallim core (depth: 145 m), composed of angular to rounded sideromelane and tachylite particles. **c**, **d** A specimen from the Jongdal core (depth: 309 m), composed generally of rounded sideromelane particles

rim, between ca. 50 and 100 m, is subtracted (Fig. 11). The absence of basement-derived accidental clasts in all cores suggests that the diatremes formed mostly within the U Formation and might have had wall angles smaller than the angle of repose, as is the case of some diatremes that formed in soft substrate environments (Lorenz 2003; Auer et al. 2007). Explosive magma-water interaction is therefore interpreted to have occurred mostly above the interface between the shelf sediment (U Formation) and the basement.

Given the known depths of some diatremes, which can be over 2.5 km deep (Lorenz 1973, 1975; Lorenz and Haneke 2004), the diatremes in this study are very shallow, probably having a shallow bowl-like geometry. Abundant shallow-level external water from multiple sources, including the interstitial water in the U Formation and the seawater that overflowed into the crater or permeated into the diatremes underground, could therefore be supplied to the diatremes to drive explosive magma-water interactions at shallow levels. The diatremes are therefore interpreted to have been kept shallow with limited downward penetration of the root zone. If the root zone of the diatremes penetrated deep into the basement rocks and sufficient access of groundwater or seawater to the explosion loci in the diatremes was prevented, the eruption style of these volcanoes might have changed from hydromagmatic to magmatic activity. The absence of deposits related to magmatic activity (lava and scoria) in the studied diatreme fills is consistent with the interpretation that the diatremes remained shallow throughout the eruption with the unexhausted supply of external water into the diatremes.

The absence of bedded upper diatreme deposits in all studied cores is also interpreted to be related to the shallowness of the diatreme structure. As the syn-eruptive crater floor deepens, the crater floor becomes the site of

pyroclastic deposition from base surges and tephra fall. These primary tephra beds, alternating with reworked tephra beds, result in the bedded upper diatreme deposits in phreatomagmatic diatremes (White and Ross 2011) and can subside to great depths of the diatremes during and after the diatreme formation (Suhr et al. 2006; Delpit et al. 2014). The absence of such bedded deposits in the studied cores suggests that the majority of the tephra ejected from the crater could be expelled out of the crater because of the low height of the crater rim relative to the syn-eruptive crater floor and the wide-angle spreading of tephra jets from the shallow diatremes. The primary diatreme fills could be therefore overlain directly by post-eruptive resedimented volcaniclastic deposits, which accumulated mostly by mass-wasting processes in a subaqueous setting in post-eruptive craters.

Hydrovolcanic activity on a continental shelf

The upper surface of the U Formation occurs about 120 m below sea level on average (Koh et al. 2017a, b, 2022), which is almost identical to the sea levels during the glacial maxima in the Quaternary (Shackleton 1987; Waelbroeck et al. 2002). The pre-eruptive surface of the subsurface volcanoes is therefore interpreted to have been submerged in sea water at a depth of about 120 m during the interglacials, almost identical to the pre-eruptive setting of Surtsey in 1963 (Thorarinsson 1967; Kokelaar 1983; Moore 1985; Jackson et al. 2019; McPhie et al. 2020; Moore and Jackson 2020), whereas it was either barely exposed above sea level or submerged in very shallow waters during the glacials. The Yellow Sea continental shelf is therefore considered to have been an optimal place for either Surtseyan or other phreatomagmatic activity because of the low hydrostatic pressure of the water column, even during the highstands of sea level, and the availability of external water for Surtseyan to phreatomagmatic explosions, either on the surface or in the subsurface. The still unconsolidated sediments of the U Formation could also facilitate efficient mixing between ascending magma and sediment. The early-stage volcanism of Jeju Island could thus be dominated by hydrovolcanic activity, which lasted more than a million years between ~ 1.88 and ~ 0.5 Ma (Koh et al. 2013, 2017a, b, 2022) until proto-Jeju Island emerged above the fluctuating Quaternary sea levels in the Middle Pleistocene (Sohn and Park 2004; Sohn et al. 2008).

Either Surtseyan or other phreatomagmatic activity is inferred to have occurred on the continental shelf, resulting in either Surtseyan tuff cones or Taalian tuff rings (Sohn et al. 2008). Judging on the basis of the general nature of hydrovolcanic activity, Surtseyan activity is supposed to have been more prevalent during the interglacials, although Surtseyan activity can occur in the glacials if abundant shallow-level groundwater is available for magma-water interactions near the surface (e.g., Hamilton and Myers 1963; Leat and Thompson 1988; Sohn and Chough 1992). Phreatomagmatic activity appears to have been possible either during the glacials or during the interglacials because explosive magma-water interaction in the subsurface and diatreme formation can occur irrespective of the presence of a water column of ca. 100 m or more above the eruption site (Leys 1983; Elliott et al. 2015). The phreatomagmatic activity associated with the diatreme of the Hankyung core is, however, interpreted to have occurred in the glacials (see below). High-resolution age data within ca. 10,000 years of error are necessary to confirm the relationship between the Quaternary sea levels and the volcano types in the subsurface.

Volcano types on the surface

The eruption styles and the volcano types on the surface associated with the subsurface diatremes are difficult to infer. However, the thinly stratified tuffs constituting the steeply inclined bedded deposits of the Hankyung core (Fig. 7a) originated most probably from the rim beds of a tuff ring surrounding the diatreme, which were emplaced by pyroclastic surges (Sohn et al. 2008). The diatreme of the Hankyung core is therefore interpreted to have been generated by phreatomagmatic explosions during a lowstand of sea level in the glacials. If the eruption occurred in the interglacials, the tuff ring could have been submergent and comprised subaqueous wave- or current-influenced facies (e.g., White 1996a). Post-eruptive crater floor appears to have been far below the pre-eruption surface, probably because of the almost complete emptying of the diatreme fill by the final eruptions. The crater could thus accommodate the fairly thick post-eruptive sediments (Fig. 11).

Similar information on the volcanic edifices on the surface is not available from the Hallim and Jongdal cores. However, the contrastingly different textures of juvenile clasts in these cores (Fig. 5) suggest that their eruptive conditions and settings were quite different. The moderately vesicular and commonly fluidally shaped clasts of the Hallim core are interpreted to have resulted from bulk interaction or coarse mixing (Kokelaar 1986) of vesiculating magma with a mobile slurry of tephra and water that were filling a shallow bowl-like or funnel-shaped vent, not far below the pre-eruption surface, whereas the sideromelane ash matrix resulted from molten fuel–coolant interaction (MFCI), which occurred in concert with the bulk interaction.

The non-vesicular and blocky/angular clasts of the Jongdal core, as well as those of the Hankyung core, resulted most likely from phreatomagmatic interaction of


a
Sm
LTs
Sm
10 cm
b
Sm
Ss
c
Ss
Shell-rich
d
Ss clast
Mm
Ss
10 cm
e
LTs

◂**Fig. 10** Features of post-eruptive deposits. **a** Thinly stratified lapilli tuff (facies LTs) overlying massive sandstone (facies Sm) in the Hallim core (depth: 128 – 129 m). **b** Massive to very crudely stratified sandstone in the Hallim core (depth: 129 – 130 m). **c** A mollusk shell-rich sand bed intercalated in a crudely stratified and poorly sorted sandstone of the Hankyung core (depth: 330 m). **d** Massive mudstone (facies Mm) containing an intraformational clast of stratified sandstone (Hallim core; depth: 125 – 126 m). **e** Crudely stratified and poorly sorted lapilli tuff from the Hankyung core (depth: 299 m)

non-vesiculated magma and water in the subsurface under higher confining pressure, involving both contact-surface steam explosivity or MFCI and cooling-contraction granulation possibly after bulk interaction of magma and wet sediment (Kokelaar 1986; Houghton and Wilson 1989; Mattsson 2010). We, therefore, interpret that the volcanic edifice associated with the diatreme in the Hallim core was a Surtseyan tuff cone. If the tuff cone was never emergent above sea level because of its eruption in the interglacials, the tuff cone might more likely be described as a Surtla-type tuff cone (Kokelaar and Durant 1983; Cas et al. 1989; Németh and Kósik 2020). On the other hand, the volcanic edifice associated with the diatreme in the Jongdal core is presumed to have been a tuff ring associated with phreatomagmatic explosions in the subsurface.

The ragged or ribbon-like clasts of the Hallim core (Fig. 5a), as well as the scoriaceous bomb-like clasts with well-preserved reentrant margins (Fig. 5c), suggest that these clasts were subject to insignificant breakage and abrasion after initial fragmentation or ductile tearing apart of magma in the diatreme, although there are cases of preservation of such clasts in pyroclastic flows and debris jets, in which particle abrasion and breakage are inferred to be active (Ross and White 2005; McClintock and White 2006; McClintock et al. 2008). The abundance of matrix and the overall matrix-supported texture throughout the core also suggests that elutriation processes by debris jets or gas jets were not active. We infer that these characteristics can be the features of relatively mild clast interactions in water-saturated and highly fluid and mobile diatreme fills. We suggest that the shallow bowl-like crater and the underlying conduit filled with such water-rich slurries can be regarded as another type of diatreme that can be distinguished from the typical "phreatomagmatic diatremes" of White and Ross (2011), let alone the controversial "kimberlite diatremes" (Stiefenhofer and Farrow 2004; Sparks et al. 2007; Wilson and Head 2007a; Wilson and Head 2007b; Cas et al. 2008; Brown et al. 2008a; Porritt et al. 2008a, b, 2008b; Brown et al. 2009; White and Ross 2011). This study of the Jeju-style diatremes and the recent studies of the Surtsey (Jackson et al. 2019; McPhie et al. 2020; Moore and Jackson 2020) show that all types of hydromagmatic volcanoes, including tuff rings, tuff cones, and maars, can have diatremes in the subsurface with different sizes, shapes, and material characteristics. The term "diatreme" thus appears to lose its meaning in classifying or distinguishing between these hydromagmatic volcano types (also see the discussion in Lorenz et al. 2016).

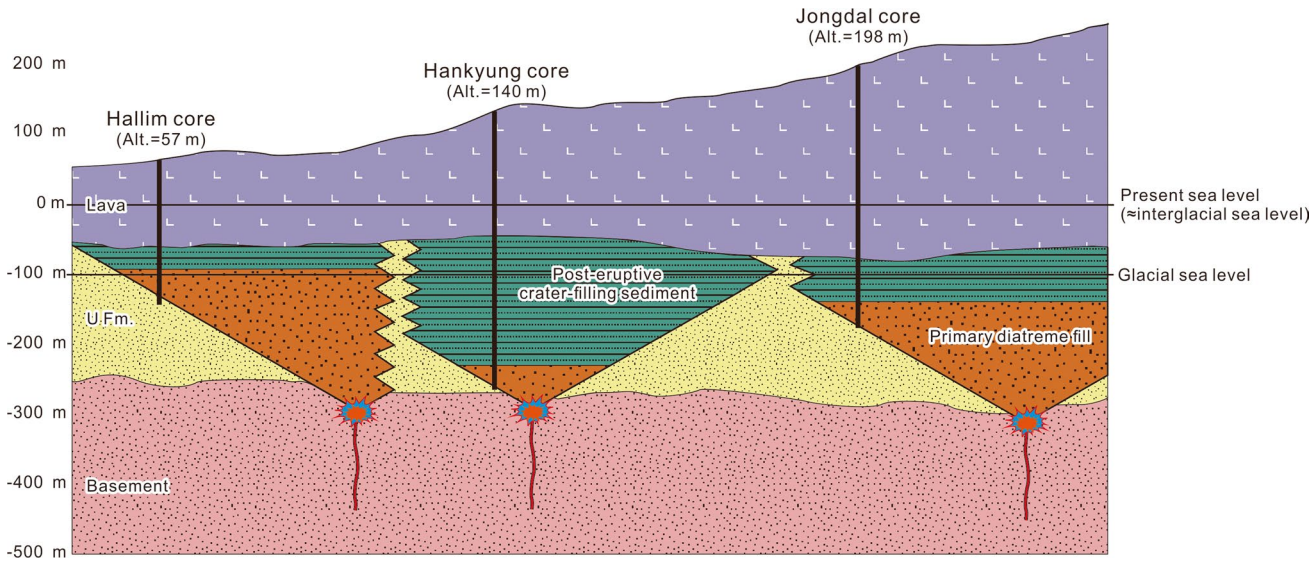

Fig. 11 Reconstruction of the diatreme position relative to the fluctuating Quaternary sea levels. No information is available regarding the diameter, wall angle, and depth of the diatremes. However, the abundance of detrital quartz sand and mudstone clasts in the diatreme deposits and the absence of basement-derived accidental lithic clasts suggest that the diatremes formed mostly within the U Formation. The wall angle of the diatremes, which is depicted as having an angle of repose (30°), can be smaller. Tuff rings/cones outside the craters are omitted for the clarity and simplicity of the diagram

Conclusions

Tens of meter-thick and massive, basaltic volcaniclastic deposits were retrieved by chance from the subsurface of Jeju Island, Korea, during groundwater drilling. They are interpreted to be either syn-eruptive diatreme-filling deposits or post-eruptive crater-filling deposits of hydromagmatic volcanoes, which formed extensively underground almost all of Jeju Island before the effusion of the lavas that built the island's present shield volcano. The pre-eruption surface of these volcanoes was a continental shelf floored by still unconsolidated sandy to muddy sediments with thicknesses between 70 and 250 m. The surface was at a depth of about 120 m below the present sea level, indicating that the surface was submerged in sea water at a depth of about 120 m during the interglacials and was either barely exposed above sea level or submerged in very shallow waters during the glacials. The setting was, therefore, optimal for either Surtseyan or other phreatomagmatic activity and the construction of either emergent or submerged tuff rings and cones.

The primary diatreme fills in three cores occur 88 m below sea level in the Hallim core, 229 m below sea level in the Hankyung core, and 135 m below sea level in the Jongdal core, suggesting that the diatremes formed mainly below the fluctuating Quaternary sea levels and that the syn-eruptive craters could be easily flooded with sea water in addition to the interstitial water seeping from the shelf sediment. The diatreme fills are devoid of basement-derived accidental lithic clasts, suggesting that the diatremes are only a few hundred meters deep and formed mostly within the shelf sediment with wall angles smaller than the angle of repose. Abundant shallow-level external water was therefore available for explosive magma-water interactions at shallow levels. The possibility of deeper explosions and disturbance of the basement rocks without the emission of the rocks to the surface cannot be ruled out. However, the basement lies fairly shallow beneath the pre-eruption surface, covered only by the unconsolidated sediment of the U Formation, which has an average thickness of 150 m (Koh et al. 2017b, 2022). The accidental lithic clasts from the basement rocks above the optimal depth of phreatomagmatic explosions (Valentine et al. 2014) are therefore inferred to be present in the diatreme fill if there were active explosions and diatreme formation in the basement.

The diatremes of these volcanoes have some features that can be attributed to extreme wetness or water saturation of the diatreme fill, such as matrix support of clasts, meager vertical changes in the matrix content, and the absence of features related to particle adhesion. Preservation of ragged to discoid shapes and delicate reentrant margins of the basalt clasts in the Hallim core is especially noteworthy because these clast textures can be the result of mild clast interactions in a water-saturated and highly fluid slurry of tephra and water that was filling a shallow funnel-shaped vent and conduit, which needs to be distinguished from both phreatomagmatic and kimberlite diatremes. In these Jeju-style diatremes, abrasion and breakage of coarse particles and elutriation of fine particles appear to occur less vigorously or less efficiently than in typical phreatomagmatic diatremes.

The volcanic edifice type on the surface is interpreted to be an emergent Surtseyan-type tuff cone or a submergent Surtla-type tuff cone in the case of the Hallim core. The eruption could have occurred either in the glacials or in the interglacials. The volcanic edifice type associated with the Hankyung core is interpreted to be a tuff ring based on the post-eruptive collapsed masses of thin-bedded tuff emplaced by pyroclastic surges. The tuff ring formed most likely in the glacials upon an emergent surface. No convincing evidence is available for the Jongdal core, but a tuff ring is likely to have formed by a phreatomagmatic eruption. High-resolution age data from these volcanoes within ca. 10,000 years of error are necessary to confirm the relationship between the Quaternary sea levels and the eruption and edifice styles.

This study suggests that a variety of diatremes with different sizes, shapes, and material characteristics can be produced beneath the craters of hydromagmatic volcanoes, including not only maars but also tuff rings and tuff cones. The term "diatreme" thus appears to lose its meaning in classifying and naming hydromagmatic volcanoes because most, if not all, hydromagmatic volcanoes can have diatremes.

Acknowledgements We thank James D. L. White and Volker Lorenz for a careful and constructive review of the paper.

Author contribution YKS contributed to the conceptualization of ideas and methodology. YJ wrote the first draft of the manuscript. YKS wrote the final version of the manuscript. All three authors contributed to sample and data collection during fieldwork. YJ and KHP contributed to the analysis and visualization of data. They also contributed to the writing process and provided feedback on data visualization.

Funding YKS is funded by the National Research Foundation of Korea (NRF-2020R1A2B5B02001660).

Data availability The datasets generated during and/or analyzed during the current study are available from the corresponding author on reasonable request.

Declarations

Ethics approval Not applicable.

Consent to participate Not applicable.

Consent for publication All authors consent to publication.

Conflict of interest The authors declare no competing interests.

References

Allen SR, Hayward BW, Mathews E (2007) A facies model for a submarine volcaniclastic apron: the Miocene Manukau Subgroup, New Zealand. Geol Soc Am Bull 119:725–742

Auer A, Martin U, Németh K (2007) The Fekete-hegy (Balaton Highland Hungary) "soft-substrate" and "hard-substrate" maar volcanoes in an aligned volcanic complex - implications for vent geometry, subsurface stratigraphy and the palaeoenvironmental setting. J Volcanol Geoth Res 159:225–245

Banerjee S, Bansal U, Vilas Thorat A (2016) A review on palaeogeographic implications and temporal variation in glaucony composition. J Palaeogeogr 5(1):43–71

Befus KS, Hanson RE, Miggins DP, Breyer JA, Busbey AB (2009) Nonexplosive and explosive magma/wet-sediment interaction during emplacement of Eocene intrusions into Cretaceous to Eocene strata, Trans-Pecos igneous province, West Texas. J Volcanol Geoth Res 181:155–172

Blair TC, McPherson JG (1998) Recent debris-flow processes and resultant form and facies of the Dolomite alluvial fan, Owens Valley. California J Sed Res 68:800–818

Bolós X, Oms O, Rodríguez-Salgado P, Martí J, Gómez de Soler B, Campeny G (2021) Eruptive evolution and 3D geological modeling of Camp dels Ninots maar-diatreme (Catalonia) through continuous intra-crater drill coring. J Volcanol Geoth Res 419: 107369

Brenna M, Cronin SJ, Kereszturi G, Sohn YK, Smith IEM, Wijbrans J (2015) Intraplate volcanism influenced by distal subduction tectonics at Jeju Island Republic of Korea. Bull Volcanol 77:7

Brown RJ, Gernon T, Stiefenhofer J, Field M (2008a) Geological constraints on the eruption of the Jwaneng Centre kimberlite pipe. Botswana J Volcanol Geoth Res 174:195–208

Brown RJ, Tait M, Field M, Sparks RSJ (2009) Geology of a complex kimberlite pipe (K2 pipe, Venetia Mine, South Africa): insights into conduit processes during explosive ultrabasic eruptions. Bull Volcanol 71:95–112

Brown RJ, Field M, Gernon T, Gilbertson M, Sparks RSJ (2008) Problems with an in-vent column collapse model for the emplacement of massive volcaniclastic kimberlite. A discussion of "In-vent column collapse as an alternative model for massive volcaniclastic kimberlite emplacement: an example from the Fox kimberlite, Ekati Diamond Mine, NWT, Canada" by Porritt et al. [J. Volcanol. Geotherm. Res. 174, 90-102]. J Volcanol Geoth Res 178:847–850

Busby-Spera CJ (1988) Development of fan-deltoid slope apron in a convergent-margin tectonic setting: Baja California, Mexico. In: Nemec W, Steel RJ (eds) Fan deltas: sedimentology and tectonic settings. Blackie, Glasgow, pp 419–429

Busby-Spera CJ, White JDL (1987) Variation in peperite textures associated with differing host-sediment properties. Bull Volcanol 49:765–775

Cas RAF, Wright JV (1987) Volcanic successions: modern and ancient. Allen and Unwin, London, p 528

Cas RAF, Landis CA, Fordyce RE (1989) A monogenetic, Surtla-type, Surtseyan volcano from the Eocene-Oligocene Waiareka-Deborah volcanics, Otago, New Zealand: a model. Bull Volcanol 51:281–298

Cas RAF, Hayman P, Pittari A, Porritt L (2008) Some major problems with existing models and terminology associated with kimberlite pipes from a volcanological perspective, and some suggestions. J Volcanol Geoth Res 174(1–3):209–225

Casalbore D, Romagnoli C, Chiocci F, Frezza V (2010) Morpho-sedimentary characteristics of the volcaniclastic apron around Stromboli volcano (Italy). Mar Geol 269:132–148

Chen XB (2007) Present-day horizontal deformation status of continental China and its driving mechanism. Sci China, Ser D Earth Sci 50(11):1663–1673

Clement CR (1982) A comparative geological study of some major kimberlite pipes in the Northern Cape and Orange Free State. Ph.D. thesis, Department of Geology, University of Cape Town, Cape Town, p 432

Delpit S, Ross P-S, B. Carter Hearn J, (2014) Deep-bedded ultramafic diatremes in the Missouri River Breaks volcanic field, Montana, USA: 1 km of syn-eruptive subsidence. Bull Volcanol 76:832

Elliott HAL, Gernon TM, Roberts S, Hewson C (2015) Basaltic maar-diatreme volcanism in the Lower Carboniferous of the Limerick Basin (SW Ireland). Bull Volcanol 77:37

Fisher RV, Schmincke H-U (1984) Pyroclastic rocks. Springer-Verlag, Berlin, Heidelberg, New York, p 472

Gernon TM, Field M, Sparks RSJ (2009) Depositional processes in a kimberlite crater: the Upper Cretaceous Orapa South Pipe (Botswana). Sedimentology 56(3):623–643

Gernon TM, Upton BGJ, Hincks TK (2013) Eruptive history of an alkali basaltic diatreme from Elie Ness, Fife. Scotland Bull Volcanol 75:704

Go SY, Kim GB, Jeong JO, Sohn YK (2017) Diatreme evolution during the phreatomagmatic eruption of the Songaksan tuff ring, Jeju Island. Korea Bull Volcanol 79:23

Hamdy AM, Park P-H, Lim H-C (2005) Horizontal deformation in South Korea from permanent GPS network data, 2000–2003. EPS 57:77–82

Hamilton WH, Myers WB (1963) Menan Buttes, cones of glassy basalt tuff in the Snake River Plain, Idaho. United States Geol Surv Professional Paper 450-E:114–118

Hanson RE, Wilson TJ (1993) Large-scale rhyolite peperites (Jurassic, southern Chile). J Volcanol Geoth Res 54:247–264

Hanson RE, Hargrove US (1999) Processes of magma/wet sediment interaction in a large-scale Jurassic andesitic peperite complex, northern Sierra Nevada. California Bull Volcanol 60:610–626

Houghton BF, Wilson CJN (1989) A vesicularity index for pyroclastic deposits. Bull Volcanol 51:451–462

Jackson MD, Gudmundsson MT, Weisenberger TB, Rhodes JM, Stefánsson A, Kleine BI, Lippert PC, Marquardt JM, Reynolds HI, Kück J, Marteinsson VT, Vannier P, Bach W, Barich A, Bergsten P, Bryce JG, Cappelletti P, Couper S, Fahnestock MF, Gorny CF, Grimaldi C, Groh M, Gudmundsson Á, Gunnlaugsson ÁT, Hamlin C, Högnadóttir T, Jónasson K, Jónsson SS, Jørgensen SL, Klonowski AM, Marshall B, Massey E, McPhie J, Moore JG, Ólafsson ES, Onstad SL, Perez V, Prause S, Snorrason SP, Türke A, White JDL, Zimanowski B (2019) SUSTAIN drilling at Surtsey volcano, Iceland, tracks hydrothermal and microbiological interactions in basalt 50 years after eruption. Scientific Drilling 25:35–46

Jeon Y, Ryu CK, Yoon W, Kang S, Song S (2013) Characteristics and interpretation of subsurface diatreme deposits from western Jeju

Island. J Geol Soc Korea 49:537–551 (in Korean with English abstract)
Jeong J-O, Yoon S-H, Koh G-W, Joe Y-J, Hong J-G, Kim J-J (2016) Mineralogical and sedimentological characteristics of the U Formation underlying the volcanic strata in Jeju Island. J Geol Soc Korea 52:389–403 (in Korean with English abstract)
Jin S, Park P-H, Park J-U (2007) Why is the South Korean peninsula largely aseismic? Geodetic evidences. Curr Sci 93:250–253
Jones DA, Wilson GS, Gorman AR, Fox BRS, Lee DE, Kaulfuss U (2017) A drill-hole calibrated geophysical characterisation of the 23 Ma Foulden Maar stratigraphic sequence, Otago, New Zealand. NZ J Geol Geophys 60:465–477
Karatson D, Németh K (2001) Lithofacies associations of an emerging volcaniclastic apron in a Miocene volcanic complex: an example from the Borzsony Mountains. Hungary Int J Earth Sci 90:776–794
Kim KH, Tanaka T, Suzuki K, Nagao K, Park EJ (2002) Evidences of the presence of old continental basement in Cheju volcanic Island, South Korea, revealed by radiometric ages and Nd-Sr isotopes of granitic rocks. Geochem J 36:421–441
Kjarsgaard BA, Wit Md, Heaman LM, Pearson DG, Stiefenhofer J, Janusczcak N, Shirey SB (2022) A review of the geology of global diamond mines and deposits. Rev Mineral Geochem 88:1–118
Koh GW (1997) Characteristics of the groundwater and hydrogeologic implications of the Seoguipo Formation in Cheju Island. Ph.D. thesis, Department of Geology, Pusan National University, Pusan, p 326
Koh GW, Park JB (2010) The study on geology and volcanism in Jeju Island (II): petrochemistry and $^{40}Ar/^{39}Ar$ absolute ages of the volcanic rocks in Gapado-Marado, Jeju Island. Econ Environ Geol 43:53–66 (in Korean with English abstract)
Koh GW, Park JB (2010) The study on geology and volcanism in Jeju Island (III): early lava effusion records in Jeju Island on the basis of $^{40}Ar/^{39}Ar$ absolute ages of lava samples. Econ Environ Geol 43:163–176 (in Korean with English abstract)
Koh GW, Park JB, Park YS (2008) The study on geology and volcanism in Jeju Island (I): petrochemistry and $^{40}Ar/^{39}Ar$ absolute ages of the subsurface volcanic rock cores from boreholes in the eastern lowland of Jeju Island. Econ Environ Geol 41(1):93–113 (in Korean with English abstract)
Koh GW, Park J-B, Moon DC (2017a) Geology and groundwater of Jeju volcanic island. Jeju Province Development Corporation, Jeju, p 262
Koh GW, Park JB, Sohn YK, Yoon SH (2017b) Guidelines for geological logging of cores of Jeju island. Jeju Province Development Corporation, Jeju, p 293
Koh GW, Park JB, Kang B-R, Kim G-P, Moon DC (2013) Volcanism in Jeju Island. J Geol Soc Korea 49:209–230 (in Korean with English abstract)
Koh GW, Kim TH, Park JB, Hong SS, Ko IJ (2019) Multiple volcanic eruption episodes in the highlands of Mt. Halla (Hallasan), Jeju Island, Korea: 40Ar/39Ar ages of lava flows. J Geol Soc Korea 55(1):71–86
Koh GW, Kim BH, Park J-B, Sohn YK, Yoon S-H, Moon DC (2022) Geomorphology and geology of Hallasan Mountain. Jeju Special Self-Governing Province, Jeju, p 333
Kokelaar BP (1983) The mechanism of surtseyan volcanism. J Geol Soc London 140:939–944
Kokelaar BP, Durant GP (1983) The submarine eruption and erosion of Surtla (Surtsey). Iceland J Volcanol Geoth Res 19:239–246
Kokelaar P (1982) Fluidization of wet sediments during the emplacement and cooling of various igneous bodies. J Geol Soc London 139:21–33
Kokelaar P (1986) Magma-water interactions in subaqueous and emergent basaltic volcanism. Bull Volcanol 48:275–289
Kwon CW, Sohn YK (2008) Tephra-filled volcanic neck (diatreme) of a mafic tuff ring at Maegok, Miocene Eoil Basin. SE Korea Geosci J 12(4):317–329
Leat PT, Thompson RN (1988) Miocene hydrovolcanism in NW Colorado, USA, fuelled by explosive mixing of basaltic magma and wet unconsolidated sediment. Bull Volcanol 50:229–243
Leckie DA, Kjarsgaard BA, Bloch J, McIntyre D, McNeil D, Stasiuk L, Heaman L (1997) Emplacement and reworking of Cretaceous, diamond-bearing, crater facies kimberlite of central Saskatchewan. Canada Geol Soc Am Bull 109:1000–1020
Leys CA (1983) Volcanic and sedimentary processes during formation of the Saefell tuff-ring, Iceland. Trans Royal Soc Edin Earth Sci 74:15–22
Liu ZX, Xia DX, Berne S, Wang KY, Marsset T, Tang YX, Bourillet JF (1998) Tidal deposition systems of China's continental shelf, with special reference to the eastern Bohai Sea. Mar Geol 145:225–253
Lorenz V (1973) On the formation of maars. Bull Volcanol 37:183–204
Lorenz V (1975) Formation of phreatomagmatic maar-diatreme volcanoes and its relevance to kimberlite diatremes. Phys Chem Earth 9:17–27
Lorenz V (1986) On the growth of maars and diatremes and its relevance to the formation of tuff rings. Bull Volcanol 48:265–274
Lorenz V (2003) Maar-diatreme volcanoes, their formation, and their setting in hard-rock or soft-rock environments. Geolines 15:72–83
Lorenz V (2008) Explosive maar-diatreme volcanism in unconsolidated water-saturated sediments and its relevance for diamondiferous pipes. Zeitschrift Der Deutschen Gemmologischen Gesellschaft 57:41–60
Lorenz V, Haneke J (2004) Relationship between diatremes, dykes, sills, laccoliths, intrusive–extrusive domes, lava flows, and tephra deposits with nconsolidated water-saturated sediments in the late Variscan intermontane Sarr-Nahe Basin, SW Germany. In: Breitkreuz C, Petford N (eds) Physical geology of high-level magmatic systems. Geological Society of London, London, pp 75–124
Lorenz V, Kurszlaukis S (2007) Root zone processes in the phreatomagmatic pipe emplacement model and consequences for the evolution of maar-diatreme volcanoes. J Volcanol Geoth Res 159(1–3):4–32
Lorenz V, McBirney AR, Williams H (1970) An investigation of volcanic depressions. Part III. Maars, tuff-rings, tuff-cones, and diatremes. In: NASA progress report (NGR 38–003–012). National Aeronautics and Space Administration, Houston, Texas, p 198
Lorenz V, Zimanowski B, Buettner R (2002) On the formation of deep-seated subterranean peperite-like magma-sediment mixtures. J Volcanol Geoth Res 114:107–118
Lorenz V, Suhr P, Suhr S (2016) Phreatomagmatic maar-diatreme volcanoes and their incremental growth: a model. In: Németh K, Carrasco-Núñez G, Aranda-Gómez JJ, Smith IEM (eds) Monogenetic volcanism, Special Publication 446. Geological Society, London
Lutz H, Lorenz V, Engel T, Häfner F, Haneke J (2013) Paleogene phreatomagmatic volcanism on the western main fault of the northern Upper Rhine Graben (Kisselwörth diatreme and Nierstein-Astheim Volcanic System, Germany). Bull Volcanol 75:741
Marsden RC, Danišík M, Ahn US, Friedrichs B, Schmitt AK, Kirkland CL, McDonald BJ, Evans NJ (2021) Zircon double-dating of Quaternary eruptions on Jeju Island. South Korea J Volcanol Geoth Res 410:107171

Martin U, Németh K (2007) Blocky versus fluidal peperite textures developed in volcanic conduits, vents and crater lakes of phreatomagmatic volcanoes in Mio/Pliocene volcanic fields of Western Hungary. J Volcanol Geoth Res 159:164–178

Mattsson HB (2010) Textural variation in juvenile pyroclasts from an emergent, Surtseyan-type, volcanic eruption: the Capelas tuff cone, São Miguel (Azores). J Volcanol Geoth Res 189:81–91

McClintock M, White JDL (2006) Large phreatomagmatic vent complex at Coombs Hills, Antarctica: wet, explosive initiation of flood basalt volcanism in the Ferrar-Karoo LIP. Bull Volcanol 68(3):215–239

McClintock M, White JDL, Houghton BF, Skilling IP (2008) Physical volcanology of a large crater-complex formed during the initial stages of Karoo flood basalt volcanism, Sterkspruit, Eastern Cape, South Africa. J Volcanol Geoth Res 172:93–111

McPhie J, White JDL, Gorny C, Jackson MD, Gudmundsson MT, Couper S (2020) Lithofacies from the 1963–1967 Surtsey eruption in SUSTAIN drill cores SE-2a, SE-2b and SE-03. Surtsey Research 14:19–32

Moore JG (1985) Structure and eruptive mechanisms at Surtsey Volcano, Iceland. Geol Mag 122:649–661

Moore JG, Jackson MD (2020) Observations on the structure of Surtsey. Surtsey Research 14:33–45

Moss S, Russell JK, Andrews GDM (2008) Progressive infilling of a kimberlite pipe at Diavik, Northwest Territories, Canada: insights from volcanic facies architecture, textures, and granulometry. J Volcanol Geoth Res 174:103–116

Mulder T, Alexander J (2001) The physical character of subaqueous sedimentary density flows and their deposits. Sedimentology 48:269–299

Nemec W, Steel RJ (1984) Alluvial and coastal conglomerates: their significant features and some comments on gravelly mass-flow deposits. In: Koster EH, Steel RJ (eds) Sedimentology of gravels and conglomerates. Calgary1–31

Németh K, Kósik S (2020) Review of explosive hydrovolcanism. Geosciences 10:44

Odin GS, Matter A (1981) De glauconiarum origine. Sedimentology 28(5):611–641

Park J-B, Park K-H, Cho D-L, Koh G-W (1999) Petrochemical classification of the Quaternary volcanic rocks in Cheju Island. Korea J Geol Soc Korea 35:253–264 (in Korean with English abstract)

Park JB (1994) Geochemical evolution of the Cheju Volcanic Island, Korea. Ph.D. thesis, Department of Geology, Yonsei University, Seoul, p 303

Park KH, Lee BJ, Kim JC, Cho DL, Lee SR, Choi HI, Park DW, Lee SR, Choi YS, Yang DY, Kim JY, Seo JY, Sin HM (2000) Explanatory note of the Jeju (Baekado, Jinnampo) sheet (1:250,000). In: Korea Institute of Geoscience and Mineral Resources, Taejon, p 59

Porritt LA, Cas RAF, Crawford BB (2008) In-vent column collapse as an alternative model for massive volcaniclastic kimberlite emplacement: an example from the Fox kimberlite, Ekati Diamond Mine, NWT. Canada J Volcanol Geoth Res 174:90–102

Porritt LA, Cas RAF, Crawford BB (2008) Reply to: Discussion by Brown. J Volcanol Geoth Res 178:851–854

Ross P-S, White JDL (2005) Mafic, large-volume, pyroclastic density current deposits from phreatomagmatic eruptions in the Ferrar large igneous province. Antarctica J Geol 113:627–649

Ross P-S, White JDL (2006) Debris jets in continental phreatomagmatic volcanoes: a field study of their subterranean deposits in the Coombs Hills vent complex. Antarctica J Volcanol Geoth Res 149:62–84

Ross P-S, White JDL, Valentine GA, Taddeucci J, Sonder I, Andrews RG (2013) Experimental birth of a maar-diatreme volcano. J Volcanol Geoth Res 260:1–12

Schipper CI, White JDL, Zimanowski B, Büttner R, Sonder I, Schmid A (2011) Experimental interaction of magma and "dirty" coolants. Earth Planet Sci Lett 303:323–336

Shackleton NJ (1987) Oxygen isotopes, ice volume and sea level. Quatern Sci Rev 6:183–190

Sheridan MF, Wohletz KH (1983) Hydrovolcanism: basic considerations and review. J Volcanol Geoth Res 17:1–29

Shinn YJ, Chough SK, Kim JW, Woo J (2007) Development of depositional systems in the southeastern Yellow Sea during the postglacial transgression. Mar Geol 239:59–82

Shultz AW (1984) Subaerial debris flow deposition in the Upper Paleozoic Cutler Formation, western Colorado. J Sed Petrol 54:759–772

Simkin T, Siebert L (1984) Explosive eruptions in space and time: durations, intervals, and a comparison of the worlds's active volcanic belts. In: Committee GS, Council NR (eds) Explosive volcanism: inception, evolution, and hazards. National Academy Press, Washington, D.C., pp 110–121

Simkin T, Siebert L (2000) Earth's volcanoes and eruptions: an overview. In: Sigurdsson H, Houghton BF, McNutt SR, Rymer H, Stix J (eds) Encyclopedia of volcanoes. Academic Press, San Diego, CA, pp 249–261

Sohn YK (1996) Hydrovolcanic processes forming basaltic tuff rings and cones on Cheju Island. Korea Geol Soc Am Bull 108(10):1199–1211

Sohn YK (2000) Coarse-grained debris-flow deposits in the Miocene fan deltas, SE Korea: a scaling analysis. Sed Geol 130(1–2):45–64

Sohn YK, Chough SK (1992) The Ilchulbong tuff cone, Cheju Island, South Korea: depositional processes and evolution of an emergent. Surtseyan-Type Tuff Cone Sedimentology 39(4):523–544

Sohn YK, Park KH (2004) Early-stage volcanism and sedimentation of Jeju Island revealed by the Sagye Borehole, SW Jeju Island. Korea Geosci J 8(1):73–84

Sohn YK, Park KH (2005) Composite tuff ring/cone complexes in Jeju Island, Korea: possible consequences of substrate collapse and vent migration. J Volcanol Geoth Res 141(1–2):157–175

Sohn YK, Rhee CW, Kim BC (1999) Debris flow and hyperconcentrated flood-flow deposits in an alluvial fan, northwestern part of the Cretaceous Yongdong basin, central Korea. J Geol 107(1):111–132

Sohn YK, Park KH, Yoon SH (2008) Primary versus secondary and subaerial versus submarine hydrovolcanic deposits in the subsurface of Jeju Island. Korea Sedimentology 55(4):899–924

Sohn YK, Sohn C, Yoon WS, Jeong JO, Yoon S-H, Cho H (2021) Volcano–air–sea interactions in a coastal tuff ring, Jeju Island, Korea. In: Di Capua A, De Rosa R, Kereszturi G, Le Pera E, Rosi M, Watt SFL (eds) Volcanic processes in the sedimentary record: when volcanoes meet the environment, Special Publication 520. Geological Society, London

Sohn YK, Yoon WS, Ahn US, Kim GB, Lee J-H, Ryu CK, Jeon YM, Kang CH (2015) Stratigraphy and age of the human footprints-bearing strata in Jeju Island, Korea: controversies and new findings. J Archaeol Sci Rep 4:264–275

Son M, Kim JS, Jung S, Ki JS, Kim MC, Sohn YK (2012) Tectonically controlled vent migration during maar-diatreme formation: an example from a Miocene half-graben basin in SE Korea. J Volcanol Geoth Res 223:29–46

Sparks RSJ, Brown RJ, Field M, Gilbertson M (2007) Kimberlite ascent and eruption. Nature 450:E21–E21

Stiefenhofer J, Farrow DJ (2004) Geology of the Mwadui kimberlite, Shinyanga district, Tanzania. Lithos 76:139–160

Suhr P, Goth K, Lorenz V, Suhr S (2006) Long lasting subsidence and deformation in and above maar-diatreme volcanoes - a never ending story. Z Dt Ges Geowiss 157(3):491–511

Tatsumi Y, Shukuno H, Yoshikawa M, Chang Q, Sato K, Lee MW (2005) The petrology and geochemistry of volcanic rocks on Jeju Island: plume magmatism along the Asian continental margin. J Petrol 46:523–553

Thorarinsson S (1967) Surtsey: the new island in the North Atlantic. The Viking Press Inc, New York, p 47

Thorarinsson S, Einarsson T, Sigvaldason G, Elisson G (1964) The submarine eruption off the Vestmann Islands 1963–1964. Bull Volcanol 27:435–445

Valentine GA, White JDL (2012) Revised conceptual model for maar-diatremes: subsurface processes, energetics, and eruptive products. Geology 40:1111–1114

Valentine GA, Graettinger AH, Sonder I (2014) Explosion depths for phreatomagmatic eruptions. Geophys Res Lett 41:3045–3051

Vespermann D, Schmincke H-U (2000) Scoria cones and tuff rings. In: Sigurdsson H, Houghton BF, McNutt SR, Rymer H, Stix J (eds) Encyclopedia of volcanoes. Academic Press, San Diego, pp 683–694

Waelbroeck C, Labeyrie L, Michel E, Duplessy JC, McManus JF, Lambeck K, Balbon E, Labracherie M (2002) Sea-level and deep water temperature changes derived from benthic foraminifera isotopic records. Quatern Sci Rev 21:295–305

Ward JF, Rosenbaum G, Ubide T, Wu J, Caulfield JT, Sandiford M, Gürer D (2021) Geophysical and geochemical constraints on the origin of Holocene intraplate volcanism in East Asia. Earth-Sci Rev 218:103624

Wentworth CK (1938) Ash formations of the Island of Hawaii. Hawaiian Volcano Observatory Special Report no. 3. U.S. Geological Survey, Denver 183

White JDL (1991a) The depositional record of small, Monogenetic volcanoes within terrestrial basins. In: Fisher RV, Smith GA (eds) Sedimentation in volcanic settings. Society for Sedimentary Geology (SEPM) 155–171

White JDL (1991) Maar-diatreme phreatomagmatism at Hopi Buttes, Navajo Nation (Arizona). USA Bull Volcanol 53:239–258

White JDL (1996) Pre-emergent construction of a lacustrine basaltic volcano, Pahvant Butte, Utah (USA). Bull Volcanol 58:249–262

White JDL (1996) Impure coolants and interaction dynamics of phreatomagmatic eruptions. J Volcanol Geoth Res 74:155–170

White JDL, Houghton BF (2006) Primary volcaniclastic rocks. Geology 34:677–680

White JDL, Ross P-S (2011) Maar-diatreme volcanoes: a review. J Volcanol Geoth Res 201:1–29

Wilson L, Head JW III (2007) An integraded model of kimberlite ascent and eruption. Nature 447:53–57

Wilson L, Head JW, IIIWilson & Head reply to Sparks, et al (2007) Nature 450:E22–E22

Wohletz K, Sheridan M (1983) Hydrovolcanic eruptions II. Evolution of basaltic tuff rings and tuff cones. Am J Sci 283:385–413

Wohletz KH, McQueen RG (1984) Experimental studies of hydromagmatic volcanism. In: Committee GS, Council NR (eds) Explosive volcanism: inception, evolution, and hazards. National Academy Press, Washington, D.C., pp 158–169

Yeo E-Y, Choi J-H, Ahn US, Cheong AC-s (2019) Quartz OSL dating of palaeosols intercalated with basaltic lava flows and scoria deposits from monogenetic volcanoes in northeastern Jeju Island. Korea Geosci J 23:881–894

Yoon S, Yi S, Bak Y-S, Jung CY, Lee E-H (2004) Calcareous nannofossils and diatoms from the groundwater monitoring wells in the eastern part of Jeju Island. J Paleontol Soc Korea 20:99–119 (in Korean with English abstract)

Zimanowski B (2001) Phreatomagmatic explosions. In: Freundt A, Rosi M (eds) From magma to tephra: modelling physical processes of explosive volcanic eruptions. Elsevier, Amsterdam, pp 25–55

Zimanowski B, Buttner R (2002) Dynamic mingling of magma and liquefied sediments. J Volcanol Geoth Res 114:37–44

Zimanowski B, Buttner R, Lorenz V, Hafele H-G (1997) Fragmentation of basaltic melt in the course of explosive volcanism. J. Geophys. Res. 102(B1):803–814

Zimanowski B, Bu¨ttner R, Dellino P, White JDL, Wohletz KH (2015) Magma-water interaction and phreatomagmatic fragmentation. In: Sigurdsson H, Houghton B, McNutt Sr, Rymer H, Stix J (eds) The encyclopedia of volcanoes, second edition. Elsevier Amsterdam 473–484

Zonneveld J-P, Kjarsgaard BA, Harvey SE, Heaman LM, McNeil DH, Marcia KY (2004) Sedimentologic and stratigraphic constraints on emplacement of the Star Kimberlite, east-central Saskatchewan. Lithos 76:115–138